Triazole-Containing [FeFe] Hydrogenase Mimics: Synthesis and Electrocatalytic Behavior

Alba D. Merinero,[†] Alba Collado,[†] Luis Casarrubios,[†] Mar Gómez-Gallego,[†] Carmen Ramírez de Arellano,[‡] Antonio Caballero,[§] Fabiola Zapata,[§] and Miguel A. Sierra*[,†]

[†]Departamento de Química Orgánica I, Facultad de Química, and Center for Innovation in Advanced Chemistry (ORFEO−CINQA), Universidad Complutense, 28040 Madrid, Spain

[‡]Departamento de Química Orgánica and Center for Innovation in Advanced Chemistry (ORFEO−CINQA), Universidad de Valencia, 46100 Valencia, Spain

[§]Departamento de Química Orgánica, Facultad de Química, Universidad de Murcia, 30100 Murcia, Spain

Supporting Information

ABSTRACT: Through a Cu-catalyzed Huisgen cycloaddition between terminal alkynes and azides (CuAAC) reaction, azide $[(\mu\text{-}SCH_2)_2N(4\text{-}N_3C_6H_4)Fe_2(CO)_6]$ has demonstrated to be a robust and versatile reagent able to incorporate the $[(\mu\text{-}SR)_2Fe_2(CO)_6]$ fragment on a wide range of substrates, ranging from aromatic compounds to nucleosides, metallocenes, or redox and luminescent markers. The $[Fe^IFe^I]/[Fe^0Fe^I]$ and $[Fe^0Fe^I]/[Fe^0Fe^0]$ reduction potentials of the triazole derivatives prepared are comparable to those of other aminodithiolate (adt) Fe−Fe hydrogenase mimics. The presence of the triazole linker influences the electrochemical behavior of these complexes depending on the strength of the acid employed.

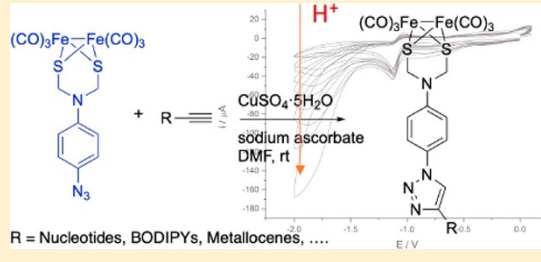

INTRODUCTION

Hydrogenases[1] are metalloenzymes able to catalyze one of the simplest reactions, the reduction of protons to form molecular hydrogen, and also the reverse process, the formation of protons and electrons from hydrogen. As it has been recognized,[2] there are two main alternatives to use enzymatic processes in the development of bulk production of hydrogen. The first one uses whole organisms, inorganic biohybrids, or supported enzymatic systems.[3] Synthetic small molecules acting as hydrogenase mimics are the second alternative to the current methods to produce hydrogen within this field of research.[4]

Mimics of the [FeFe] hydrogenases (Figure 1) have been profusely studied during the last years due to the structural similarity between the active center of such enzymes and $[(\mu\text{-}SR)_2Fe_2(CO)_6]$ complexes. Modifications of this basic structure allowed to prepare [FeFe] biomimetics having low and reversible reduction potentials (between 0 and −2.20 V in polar media) and stable enough to be used as catalysts for hydrogen production.[4]

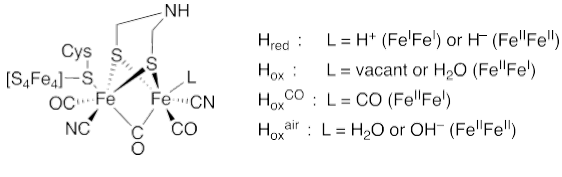

Figure 1. Active center of an [FeFe] hydrogenase.

Several variations of this basic biomimetic motif have been reported, including, among others, the incorporation of the electron source into the [FeFe] nucleus,[5] supramolecular self-assembly,[6] or direct electron transfer using Si-containing [FeFe] nuclei.[7]

Generally, the preparation of [FeFe] biomimetics relies on two different approaches to incorporate the bridging dithiolate ligand to the [FeFe] core.[4i] The first one (Scheme 1a) begins with a primary amine, which is incorporated to the $[Fe_2(CO)_6]$

Scheme 1. Approaches to Incorporate the Bridging Dithiolate Ligand to the [FeFe] Nucleus of Hydrogenase Mimics

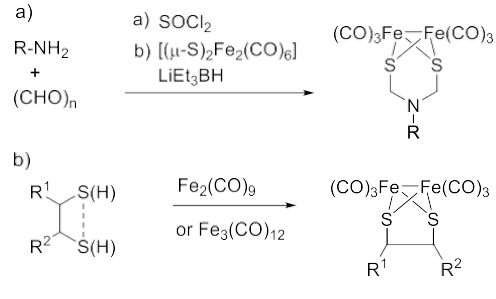

Received:
Published:

moiety by sequential formylation, chlorination, and reaction with $[(\mu\text{-S})_2Fe_2(CO)_6]Li_2$. These structures, having an azadithiolate (adt) moiety bridging between the two metal centers, are mimics of the [Fe−Fe] hydrogenase active center. Alternatively, nonamino-bridged derivatives can be prepared by reaction of 1,2-dithiols or disulfides with $Fe_2(CO)_9$ or $Fe_3(CO)_{12}$ (Scheme 1b).

These approaches are versatile and allow the preparation of sophisticated structures, but they are not able to introduce the [FeFe] moiety in sensitive molecules or in substrates having different reactive functional groups. The Cu-catalyzed Huisgen cycloaddition between terminal alkynes and azides (CuAAC)[8] is compatible with sensitive substrates and tolerates several functional groups. Our previous experience with the use of this reaction with polyfunctionalized structures and biomolecules has allowed us to prepare different organometallic-based compounds.[9]

Considering these premises, we devised the opportunity of using the CuAAC approach as a versatile way to introduce the $[(\mu\text{-SR})_2Fe_2(CO)_6]$ moiety on different substrates, employing the azide $[(\mu\text{-SCH}_2)_2N(4\text{-N}_3C_6H_4)Fe_2(CO)_6]$ (1) as a building block. This approach to make sophisticated [FeFe] hydrogenase mimics has not been yet reported and could be an easy entry to the preparation of a wide range of hydrogenase biomimetics bearing multifunctional substrates such as nucleobases, multimetallic systems, or fluorescent labels.[10]

RESULTS AND DISCUSSION

Azide 1 was prepared in 64% overall yield by condensation of *p*-azidoaniline with *p*-formaldehyde, isolation of the intermediate hexahydro-1,3,5-*p*-azidophenyl-*s*-triazine 2, and subsequent reaction with $[(\mu\text{-SH})_2Fe_2(CO)_6]$ (generated in situ by reaction of $[(\mu\text{-S}_2Fe_2(CO)_6]$ with $LiEt_3BH$, followed by treatment of the lithium salt with trifluoracetic acid (TFA) in tetrahydrofuran (THF)) (Scheme 2). Crystals of 1 were grown from CH_2Cl_2/hexane, and the structure was established by NMR spectroscopy and X-ray diffraction analysis (see Supporting Information for details). As a proof of concept, we first tested the reaction of azide 1 with a simple, unfunctionalized alkyne 3a. The reaction proceeded in the presence of $CuSO_4 5H_2O$ and sodium ascorbate, at room temperature (rt), affording the triazole 4a as a single reaction product (75% yield after flash chromatography). The structure was established by ^{1}H NMR spectroscopy, which showed the characteristic triazole CH signal at 8.09 ppm together with the signal corresponding to the SCH_2 groups at 4.38 ppm. Full confirmation of the 1,4-regiochemistry of the triazole ring was obtained by X-ray diffraction analysis (see below). Therefore, azide 1 bearing the $[(\mu\text{-SCH}_2)_2N(Ar)Fe_2(CO)_6]$ moiety tolerates the reducing conditions required for the standard CuAAC procedure. Once the viability of our approach was confirmed, we studied the reactivity of azide 1 with alkyne 3b having an additional basic center. The resulting triazole 4b was obtained in 80% isolated yield (Scheme 3).

Scheme 2. Synthesis of Azide 1 and X-ray Determination of the Structure of 1

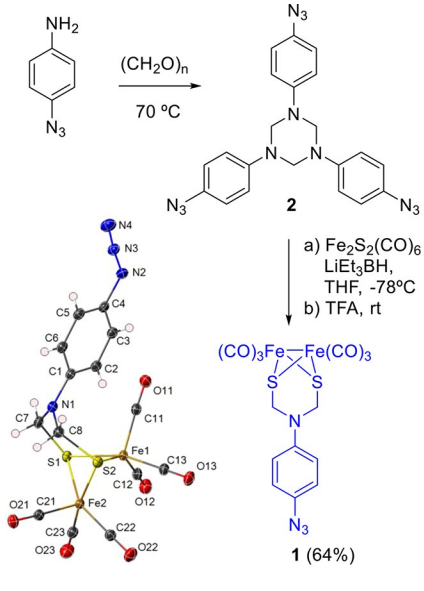

Scheme 3. Synthesis of Triazoles 4a and 4b

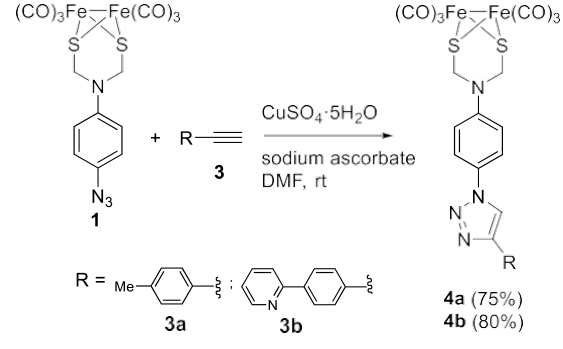

The possibility of incorporating the $[(\mu\text{-SR})_2Fe_2(CO)_6]$ moiety into a nucleobase scaffold to form mixed nucleobase/$[(\mu\text{-SR})_2Fe_2(CO)_6]$ derivatives was studied next.[11] Thus, azide 1 was reacted under the CuAAC conditions mentioned above, with purine 5a (prepared from 6-chloro-9-octyl purine by sequential Sonogashira coupling with trimethylsilylacetylene, 85% yield), followed by removal of the trimethylsilyl (TMS) group (tetra-*n*-butylammonium fluoride (TBAF), THF, rt, 51%), to yield triazolyl-derivative 6a in 43% isolated yield. In a similar way, reaction of azide 1 with ethynylphenylpurine 5b (obtained by reaction of 6-chloro-9-ethylpurine and tributyl 4-[2-(trimethylsilyl)ethynyl]phenyl]tin, 73% yield) and subsequent removal of the TMS group (68% yield) led to the corresponding triazole 6b in 97% isolated yield (Scheme 4). The synthesis of modified nucleosides was next addressed. Thus, acetylated purine derivatives 5c and 5d were reacted with azide 1 under the above CuAAC conditions to yield triazole nucleosides 6c and 6d in 55% and 85% isolated yields, respectively. Analogously, pyrimidine derivative 7 formed triazole 8 in 78% yield (Scheme 4). It is worth noting that sensitive sugar moieties as well as polybasic purine and pyrimidine heterocyclic moieties were fully compatible with the procedure.

To complete the scope of the reaction of azide 1 with nucleobases, 6-phenylpurine 9, having a 9-butinyl moiety, was reacted with 1 to yield 10 (82%) (Scheme 5). The structure of complex 10 was confirmed by X-ray diffraction analysis of a crystal grown from a concentrated dimethylformamide (DMF) solution (Figure 2).

Both molecular structures of 1 (Scheme 2) and 10 show $[(\mu\text{-SR})_2Fe_2(CO)_6]$ type of complexes with a [2Fe-2S] cluster adopting a butterfly geometry. In the structures, each iron

Scheme 4. Synthesis of Purine and Pyrimidine Derivatives 6a−6d and 8

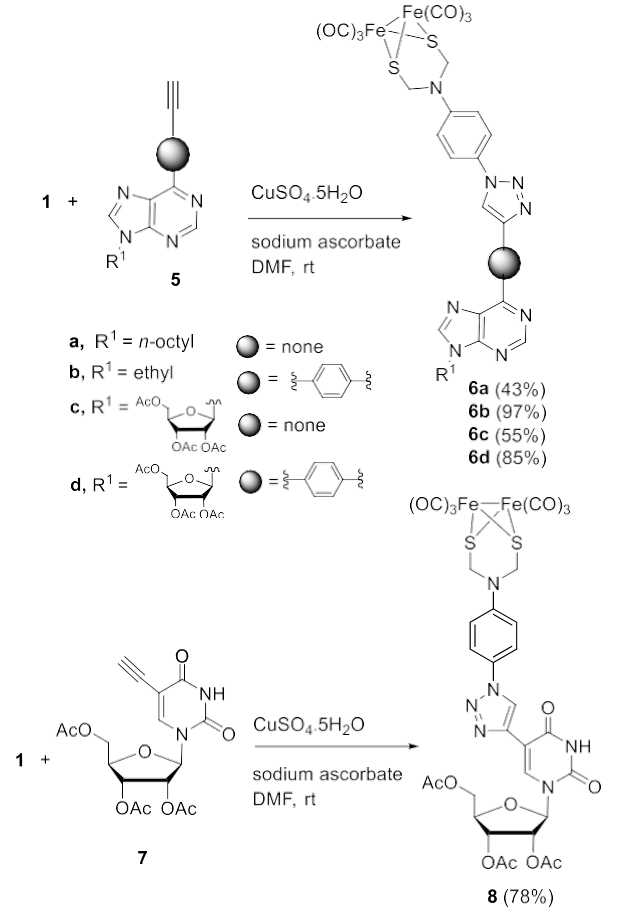

Scheme 5. Synthesis of Nucleobase Derivative 10 Containing the $[(\mu\text{-SR})_2Fe_2(CO)_6]$ Moiety

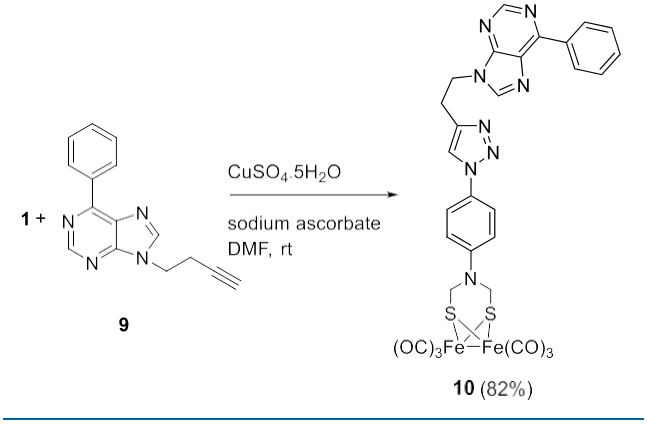

atom is bonded to both bridging dithiolate sulfur atoms and three carbonyl groups, showing a distorted square-pyramidal environment. The Fe−Fe bond lengths for 1 (2.5041(3) Å) and 10 (2.5056(10) Å) lie in the range found for similar hexacarbonyl azadithiolate diirion structures (2.486−2.588 Å).[12] Fe−Fe bond lengths for 1 and 10 are shorter than those found in the structures of metalloenzymes hydrogenase DdI (ca. 2.55 Å) or CpI (ca. 2.62 Å).[13] In compounds 1 and 10, the *N*-substituted aza disul*fi*de bridging ligand and both iron atoms form two fused six-membered metallocycles. For both structures the metallocycle corresponding to Fe(1) adopts a

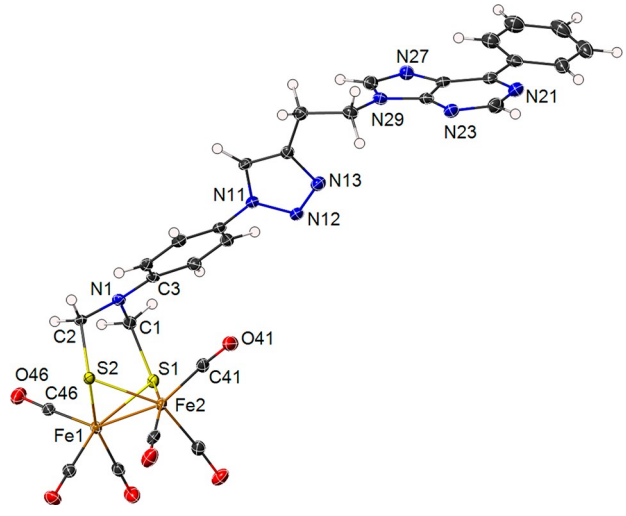

Figure 2. X-ray thermal ellipsoid plot for compound 10 (50% probability level). Selected bond lengths (Å) and angles (deg): Fe(1)−Fe(2) 2.5056(10), Fe(1)−C(46) 1.790(5), Fe(1)−C(45) 1.807(5), Fe(1)−C(44) 1.808(5), Fe(1)−S(1) 2.2640(14), Fe(1)−S(2) 2.2670(12), Fe(2)−C(42) 1.799(5), Fe(2)−C(43) 1.805(5), Fe(2)−C(41) 1.811(5), Fe(2)−S(2) 2.2639(12), Fe(2)−S(1) 2.2704(14), N(1)−C(3) 1.409(6), N(1)−C(1) 1.435(6), N(1)−C(2) 1.440(6), N1 C2 1.440(6), C(46)−Fe(1)−C(45) 100.3(2), C(46)−Fe(1)−C(44) 97.7(2), C(46)−Fe(1)−S(1) 103.34(17), C(46)−Fe(1)−S(2) 99.18(15), S(1)−Fe(1)−S(2) 85.10(5), C(46)−Fe(1)−Fe(2) 146.68(17), C(41)−Fe(2)−S(2) 111.68(15), C(41)−Fe(2)−S(1) 104.90(17), S(2)−Fe(2)−S(1) 85.02(5), C(41)−Fe(2)−Fe(1) 156.14(17), Fe(1)−S(1)−Fe(2) 67.09(4),Fe(2)−S(2)−Fe(1) 67.15(4), C(3)−N(1)−C(1) 120.5(4), C(3)−N(1)−C(2) 120.6(4), C(1)−N(1)−C(2) 112.1(4).

chair conformation with the nitrogen substituent N-R group bending toward the Fe(2) atom. Correspondingly, the metallacycle involving the Fe(2) atom adopts a boat conformation with Fe(2)·N(1) distances of 3.472(1) and 3.481(4) Å for compounds 1 and 10, respectively. The amino nitrogen atom N(1) has not a planar geometry but shows a C−N−C angle sum of 355.6(1)° for compound 1 and 353.2(4)° for compound 10, with the *N*-R group on an axial position for both metallacycles. This unexpected conformation implies short intramolecular distances between both the amino nitrogen atom N(1) and the *C*-ipso of the N-arene group with the closest carbonyl group [1: N(1)·C(21) 3.525(2) and C(31)·C(21) 3.221(2) Å; 10: N(1)·C(41) 3.609(7) and C(3)·C(41) 3.1563 Å]. Furthermore, the *N*-arene mean plane is almost parallel to the closest carbonyl bond [1: 2.6° and 10: 3.5°]. This has been previously described as a long-range interaction between the arene group and the closest carbonyl group, which produces an enlargement on the C−Fe−Fe angle for the implicated carbonyl group.[4c,14] Thus, for compound 1 the C(21)−Fe(2)−Fe(1) angle is 7.33(4)° larger than the C(11)−Fe(1)−Fe(2) angle, and, for compound 10, the C(41)−Fe(2)−Fe(1) angle is 9.46(17)° larger than the C(46)−Fe(1)−Fe(2) angle.[15]

The ORTEP diagram of complex 10 in Figure 2 con*fi*rms the presence of a 1,4-disubstituted 1,2,3-triazole moiety and by extension allows the assignment of the triazole regiochemistry in compounds 4, 6, and 8. As a matter of fact, purine and pyrimidine derivatives 5c, 5d, 8, and 10 are the *fi*rst reported bio-organometallic nucleobases containing the electroactive $[(\mu\text{-SR})_2Fe_2(CO)_6]$ moiety, which could be of relevance not

only in the electrocatalytic reduction of acids but also as a novel redox labeling in nucleobases[16] and in DNA redox damage studies.[17,18]

Luminescent boron-dipyrromethenes (BODIPYs) are other interesting substrates to be combined with the [(μ-SCH$_2$)$_2$N-(Ar)Fe$_2$(CO)$_6$] moiety. The BODIPY moiety is an essential feature in several optoelectronic devices, and it is widely used as a luminescent biomarker.[19] Thus, alkynyl-BODIPY 11 was reacted with azide 1 in the above conditions, to yield triazole 12 (39% isolated yield), as an air-stable compound (Scheme 6). Compound 12 combines the redox-active [(μ-SR)$_2$Fe$_2$(CO)$_6$] moiety with a luminescent BODIPY, which could be used as a tag in the study of mechanistic issues related to the hydrogen production using hydrogenase mimics.

Scheme 6. Synthesis of BODIPY Derivative 12 Containing the [(μ-SR)$_2$Fe$_2$(CO)$_6$] Moiety

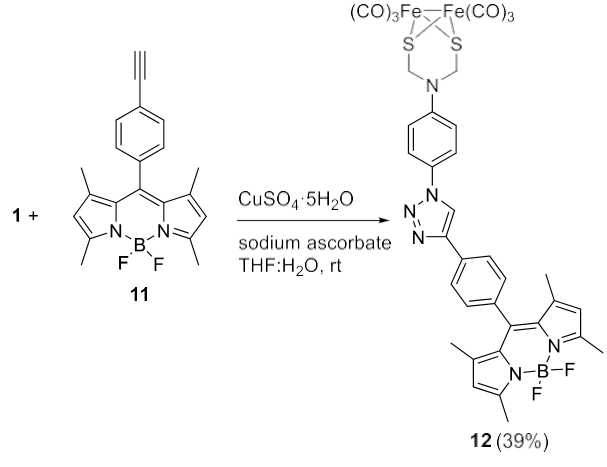

The compatibility of the CuAAC procedure involving azide 1 to prepare molecules having additional metallic centers was tested by incorporating different ethynyl sandwich and half-sandwich complexes to the [(μ-SR)$_2$Fe$_2$(CO)$_6$] moiety. In this regard, reaction of azide 1 with ethynyl ferrocene 13a, ethynyl ruthenocene 13b, and ethynylcymantrene 13c led to the desired triazole derivatives 14a−14c in good yields and as air-stable compounds (Scheme 7). Compounds 14 are interesting hetero-trimetallic products incorporating an extra redox-active fragment in their structures.

Finally, to complete the scope of the reactivity of azide 1, we attempted the preparation of the tetrametallic compound 16 by reaction of 1 with [(μ-SCH$_2$)$_2$N(Ar)Fe$_2$(CO)$_6$] alkyne 15. The reaction of these two [FeFe] components led to the tetrametallic product 16 in 83% isolated yield under the standard reaction conditions. The reaction opens the door to the preparation of molecules containing several [FeFe] cores in a single synthetic operation (Scheme 8).

Scheme 7. Synthesis of Heterotrimetallic Compounds 14a−14c Having the [(μ-SR)$_2$Fe$_2$(CO)$_6$] Moiety

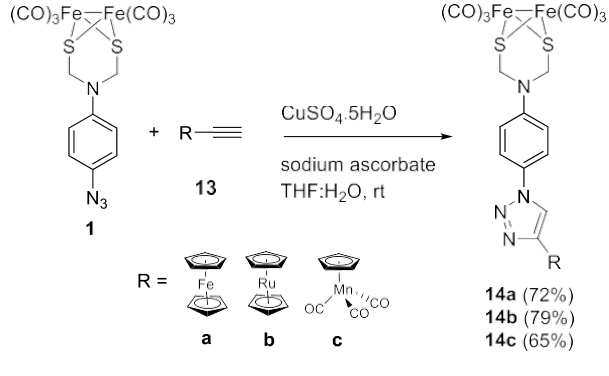

Scheme 8. Synthesis of Tetrametallic Compound 16 Containing Two [(μ-SR)$_2$Fe$_2$(CO)$_6$] Moieties

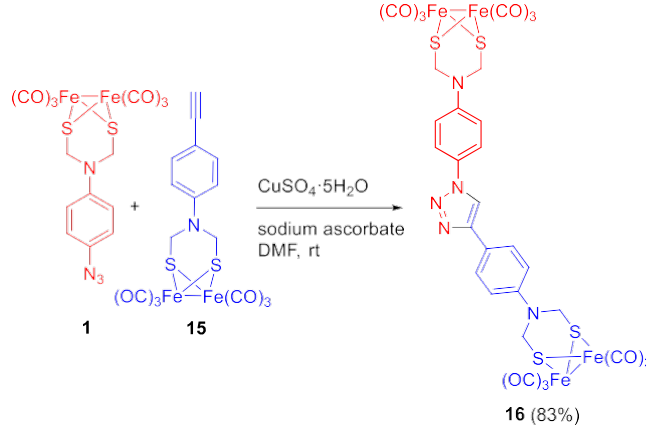

The wide scope of the reactions described above demonstrates the power of the azide 1 as a building block to produce molecular diversity in the incorporation of the [(μ-SR)$_2$Fe$_2$(CO)$_6$] moiety into many different types of compounds, which could be of relevance in the development of new hydrogenase mimics.

Electrochemistry. Cyclic voltammograms of the compounds made were recorded in CH$_3$CN solution versus Ag/AgCl (3M). Figure 3 for 4a is representative. All the compounds show an irreversible oxidation wave from ca. +0.95 to +1.04 V ascribed to the [Fe^{I}Fe^{I}]/[Fe^{II}Fe^{I}] process.[14,20,21] Metallocene compounds 14a−14c also show a wave at +0.51, +0.83, and +1.26 V, respectively, assignable to the oxidation of the additional redox-active metal center already present in the structure (see Table 1 and Figure S3 in the Supporting Information for details). In reduction, all

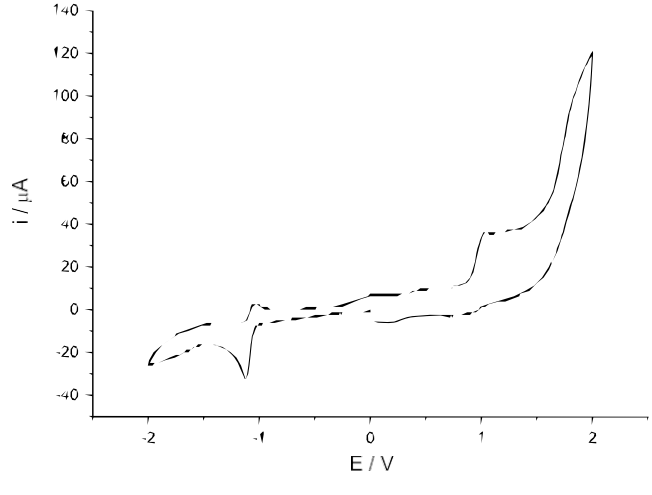

Figure 3. Cyclic voltammogram of compound 4a (10^{-3} M in CH$_3$CN, 10^{-1} M [NBu$_4$]ClO$_4$).

Table 1. Electrochemical Data of Some Representative Compounds Prepared in This Work[a]

compound	E_{pc1}	reduction[b] E_{pa1}	E_{pc2}	oxidation[b]
4a	−1.12	−1.04	−1.60	0.98
6c	−1.12	−1.02	−1.63	0.98
8	−1.15	−1.04	−1.65	0.97
12	−1.13	−1.06	−1.59	0.95
14a	−1.12	−1.01	−1.57	1.04
17[c]	−1.05	−1.00	−1.59	0.99
18[d]	−1.11	−1.03	−1.41	0.96
Me4a$^+$	−1.08	−0.98	−1.65	1.04

[a]Cyclic voltammograms of [Fe−Fe] derivatives, 10^{-3} M in CH_3CN 10^{-1} M $[NBu_4]ClO_4$, counter electrode: Pt; working electrode: glassy carbon; reference electrode: Ag/AgCl; scan rate: 100 mV/s; values given in volts. [b]The $E_{1/2}$ Fc/Fc$^+$ is 0.48 V under these conditions, and therefore the herein half-wave oxidation/reduction potentials are converted to Fc/Fc$^+$ by subtracting/adding 0.48 V from Ag/AgCl values. [c]For the synthesis of 17 see ref 14. [d]For the synthesis of 18 see ref 24.

compounds show a quasi-reversible peak from ca. −1.12 to −1.15 V, assigned to a one-electron $[Fe^IFe^I]/[Fe^0Fe^I]$ process, and a second irreversible reduction wave from ca. −1.57 to −1.65 V corresponding to the $[Fe^0Fe^I]/[Fe^0Fe^0]$ process.[14,20,21]

A rotating-disk voltammetry performed on compound 4a (1 mM, in CH_3CN) at 100 mV s^{-1} and 1000 rpm using $[(n\text{-}Bu)_4N]ClO_4$ as supporting electrolyte confirmed a 1:1 ratio (ΔI = 100 μA) of the two electrochemical processes, one of them corresponding to the first reduction $[Fe^IFe^I]/[Fe^0Fe^I]$ and the other to the oxidation $[Fe^IFe^I]/[Fe^{II}Fe^I]$ (Figure 4a). To calculate the number of electrons involved in the processes, chrono-coulombimetry experiments on compound 4a (n = 1.17 × 10^{-4} mol in 10 mL of CH_3CN) were performed, using a voltage of E = 1100 mV. A current of 1.26 C was obtained (Figure 4b), which is in agreement with a one-electron process (theoretical charge value 1.13 C).

Reduction potentials of [2Fe2S] complexes are used as key data to establish their ability to act as hydrogenase mimics for H_2 generation. For aminodithiolate (adt) derivatives, the importance of the bridgehead nitrogen for catalysis has been well-established, and not only the type of the Fe-ligands but also the electronic and structural effects of the substituents in the dithiolate bridge were claimed to be determinant to influence the electron density at the iron core.[20,21] The effect of the substituent X in the aromatic ring in adt derivatives $[(\mu\text{-}SCH_2)_2N(C_6H_4X)Fe_2(CO)_6]$ has been thoroughly studied. The presence of electron-withdrawing groups always results in a noticeable change of the reduction potentials to more positive values.[14] In this regard, and compared to the p-nitro derivative $[(\mu\text{-}SCH_2)_2N(C_6H_4NO_2)Fe_2(CO)_6]$ (17), the $[Fe^IFe^I]/[Fe^0Fe^I]$ reduction potentials of the compounds prepared through this work are ∼60 mV more negative, their values being more similar to those of halo-derivatives[20f] (i.e., p-iodo derivative $[(\mu\text{-}SCH_2)_2N(C_6H_4I)Fe_2(CO)_6]$ (18). Moreover, the experimental data in Table 1 also show that the electrochemical events are little affected by the substituents in the triazole ring, which implies that the compounds made are able to maintain the redox properties of the adt-[Fe−Fe] core, regardless the complexity of the structure linked in the CuAAC process.

The electrocatalytic response of [2Fe2S] complexes in reduction of protons is used to evaluate their activity for H_2 production.[22] The reduction of a weak acid (acetic acid, HOAc) by the triazole derivatives prepared was tested with 4a in CH_3CN as solvent. Figure 5 shows the cyclic voltammograms of 4a in the presence of increasing amounts of HOAc (0−10.0 equiv of H^+) in CH_3CN (see also Figures S15 and S16 in the Supporting Information). Under these experimental conditions, acetic acid (pK_a in MeCN = 23.5)[23] is reduced at a potential of −2.1 V in the absence of the Fe−Fe complex (see Figure S14 in the Supporting Information). The height of the

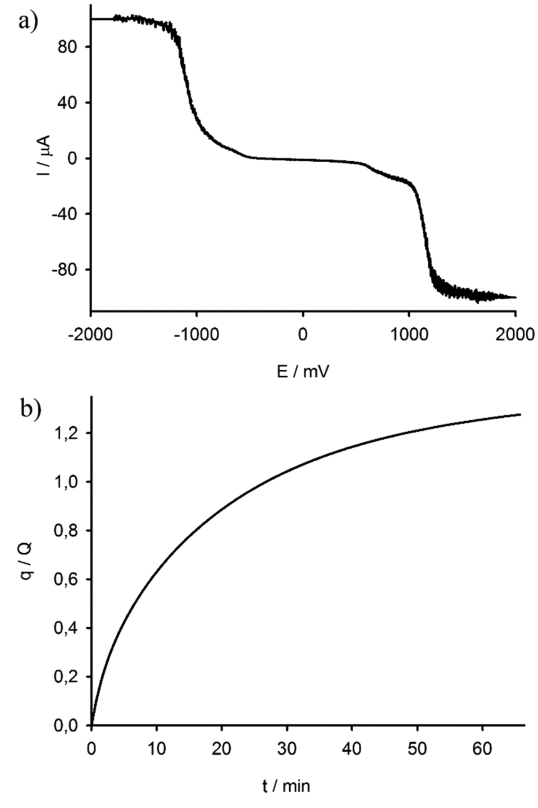

Figure 4. (a) Linear sweep voltammogram for compound 4a (1 mM), in CH_3CN using $[(n\text{-}Bu)_4N]ClO_4$ as supporting electrolyte obtained using rotating disk electrode at 100 mV s^{-1} and 1000 rpm from −2000 to 2000 mV. (b) Chrono-coulombimetric curve of the compound 4a at E = 1100 mV.

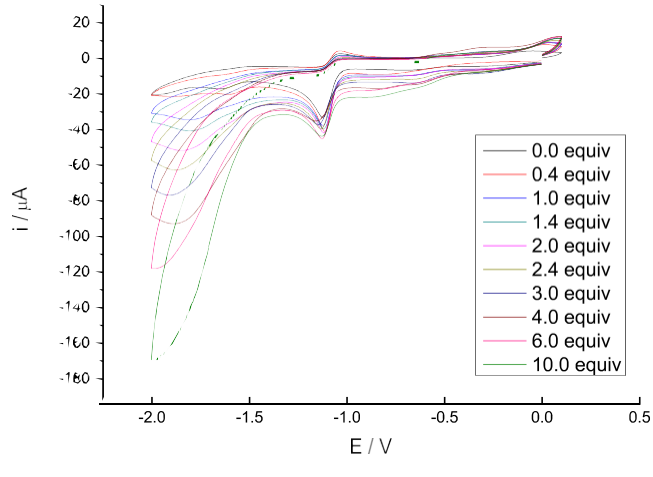

Figure 5. Cyclic voltammograms of 4a (1.0 mM) with AcOH (0.0−10.0 equiv of H^+).

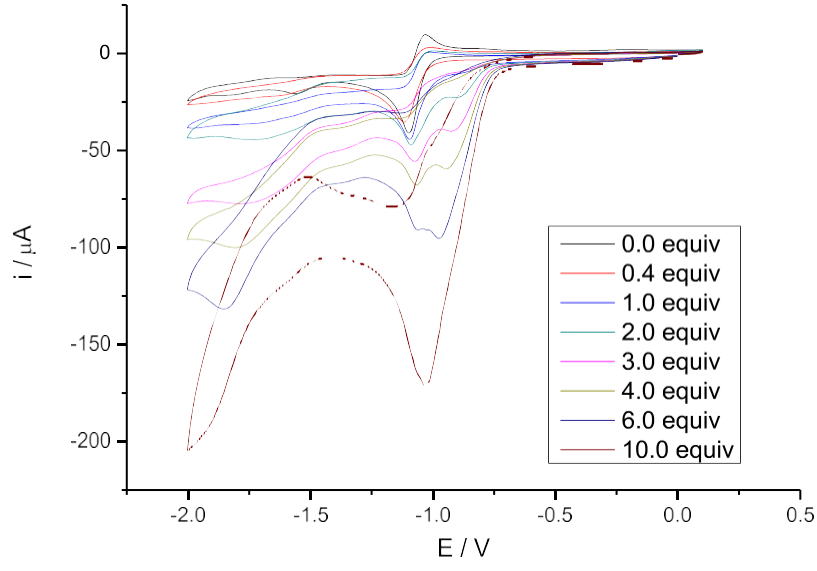

Figure 6. Cyclic voltammograms of 4a (1.0 mM) in acetonitrile, with H_2SO_4 (0.0−10.0 equiv of H^+).

reduction peak at −1.60 V continuously increases with the concentration of HOAc, indicating electrocatalytic production of H_2 by the species formed from the $[Fe^0Fe^I]/[Fe^0Fe^0]$ reduction process.[22] Interestingly, the *first* reduction event at −1.12 V assigned to the $[Fe^IFe^I]/[Fe^0Fe^I]$ process is hardly a*ff*ected by the successive additions of acetic acid: neither anodic shift nor substantial increase of the current intensity is observed.

These results contrast with those reported for other adt-bridged-[2Fe2S] derivatives, in which the *first* reduction peak is deeply a*ff*ected by the successive additions of HOAc showing both an increase in intensity and an anodic shift.[14,22a−e] In these cases, the electrocatalytic behavior with HOAc was explained by initial protonation of the nitrogen atom of the tertiary bridged amine to form $[Fe^IFe^I(NH)^+]$ species and subsequent electrolytic acid reduction of this species.[14] However, our data with HOAc in Figure 5 suggest that the protonation of the amine in the adt bridge in complex 4a must be hampered and that the catalytically active species is formed after the second $[Fe^0Fe^I]/[Fe^0Fe^0]$ reduction event. In this regard, 4a behaves more like carbon chain-bridged pdt-[2Fe2S] complexes (pdt = $S-CH_2-CH_2-CH_2-S$).[21c,d,25] The experimental results suggest that the triazole ring exerts some in*fl*uence on the mechanism of the electrocatalytic reaction of compound 4a in acidic medium. A reasonable hypothesis to explain the behavior of 4a with HOAc may be the competitive protonation of the triazole N3 nitrogen atom in preference to the bridging amino group.

To support this hypothesis ^1H NMR experiments with 4a and increasing amounts of acetic acid (1−10 equiv) were performed. Neither protonation of the triazole ring (monitored by the chemical shift of the triazole hydrogen at 8.83 ppm in acetone-d_6) nor alteration of chemical shifts of the signal of the bridging methylenes was observed (see Figure S25 in the Supporting Information).

The electrocatalytic reduction of a strong acid (H_2SO_4) by 4a was next studied (Figure 6 and Figures S17 and S18 in the Supporting Information). As the concentration of sulfuric acid increased, a new reduction event at −0.91 V (upon addition of 2.0 equiv of H^+) was clearly visible. The intensity of this new reduction wave enlarged with the successive additions of acid, whereas the initial peak at −1.12 V clearly diminished, to *fi*nally lead to a single intense peak at −1.03 V (upon addition of 10.0 equiv of H^+). Therefore, the protonation of at least one of the nitrogen atoms (either of the 1,2,3-triazole or the bridging amine) of 4a could be occurring. To support this hypothesis, ^1H NMR experiments of 4a with increasing amounts of sulfuric acid (1−10 equiv of H^+) were performed. Clear protonation of the triazole ring was observed (monitored by the displacement of the chemical shift of the triazole hydrogen from 8.83 to 9.53 ppm in acetone-d_6), while the displacement of the bridging methylenes remains unaltered (Figure S26 in the Supporting Information).

To shed some light into the proposed protonation of the compound 4a in the electrocatalytic reduction of a strong acid (H_2SO_4) we prepared triazolium salt $Me4a^+$ as a model for the protonated triazole ring of 4a. Salt $Me4a^+$ was prepared in 60% yield by reaction of 4a with Me_3OBF_4 in CH_2Cl_2 at room temperature (Scheme 9). The cyclic voltammetry of $Me4a^+$ is

Scheme 9. Synthesis of Triazolium Salt $Me4a^+$

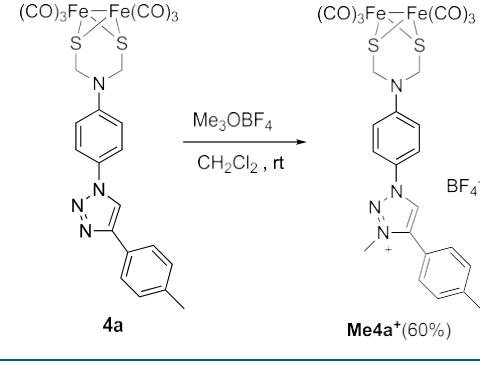

similar to that of the triazole derivatives (data in Table 1), showing two reduction events at −1.08 V (quasi-reversible) and −1.65 V (irreversible) and an irreversible oxidation wave at +1.04 V (see also Figure S19 in the Supporting Information).

The electrochemical response of triazolium salt $Me4a^+$ was studied in both HOAc and H_2SO_4. First, the protonation of $Me4a^+$ with increasing amounts of HOAc (1−10 equiv of H^+)

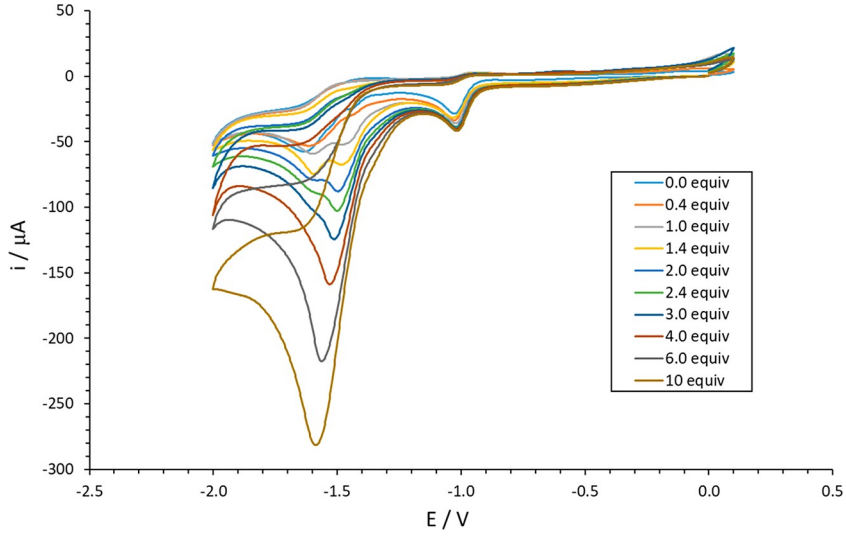

Figure 7. Cyclic voltammograms of Me4a$^+$ (1.0 mM) in acetonitrile with AcOH (0.0−10.0 equiv of H$^+$).

was checked by ^{1}H NMR (see Figure S27 in the Supporting Information). The results were similar to those obtained with triazole 4a, indicating that the protonation of the bridging amino group is probably not occurring. In agreement, the electrochemistry of Me4a$^+$ in the presence of successive amounts of HOAc showed that the first reduction event at −1.08 V was hardly affected, similar to that of 4a (Figure 7). However, as the concentration of acid increased, a new electrochemical event at −1.60 V was clearly observed.

In the presence of H_2SO_4, the behavior of Me4a$^+$ is different (Figure 8). The reduction peak at −1.08 V not only grows with

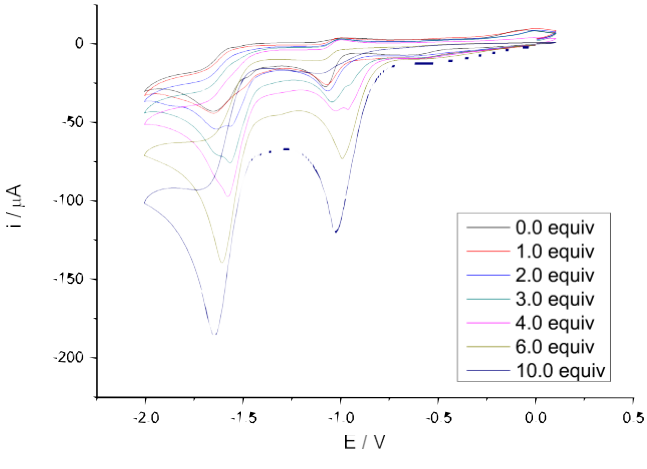

Figure 8. Cyclic voltammograms of Me4a$^+$ (1.0 mM) in acetonitrile, with H_2SO_4 (0.0−10.0 equiv of H$^+$).

increased acid concentrations but also a new reduction event at −0.96 V is clearly observed. The two bands combine to a single one at high concentration of acid. This behavior is similar to that of 4a in H_2SO_4 (Figure 6). Additionally a band at −1.60 V is also observed with increasing amounts of acid. Overall, the experimental results point to the protonation of the triazole ring in strong acid medium in preference to the adt-amino group.

Although the mechanisms for electrochemical catalysis of proton reduction by adt-bridged all-carbonyl-[Fe−Fe] model complexes are believed to occur by initial protonation of the amino bridge, the results in the derivatives prepared through this work suggest that this assumpion may be not always true. The triazole ring in 4a is playing a relevant role in the electrochemical response of the complex in acid media.

CONCLUSIONS

Azide $[(\mu\text{-}SCH_2)_2N(4\text{-}N_3C_6H_4)Fe_2(CO)_6]$ (1) is a versatile synthon able to incorporate the [2Fe2S] fragment in a wide range of molecules including nucleosides, redox indicators, and luminescent markers and, therefore, able to produce molecular diversity in these hydrogenase mimics. The electrochemical studies of the compounds prepared indicate that they maintain the redox properties of the adt-[Fe−Fe] core, regardless of the complexity of the structure linked by means of the CuAAC process.

The incorporation of the triazole ring in the structure of the [Fe−Fe] model complexes prepared deeply influences their electrocatalytic behavior in the presence of acids compared to other adt-bridged all-carbonyl derivatives. The experimental results obtained with 4a and triazolium salt Me4a$^+$ (a model for the complex 4aH$^+$) indicate that the protonation of the bridged amino group does not occur in a weak acid (HOAc), whereas in strong acid (H_2SO_4), the nitrogen atom of the triazole ring is protonated in preference.

Therefore, we can conclude that the triazole ring incorporated in the structure of the [Fe−Fe] complexes 4 prepared through this work is noninnocent in their electrocatalytic behavior in the presence of acids. Moreover, we have demonstrated that azide 1 is a key piece to produce different hydrogenase mimics, even including sensitive moieties, in a simple and effective way.

EXPERIMENTAL SECTION

General Information. Unless noted otherwise, all manipulations were performed under an argon atmosphere using standard Schlenk techniques. THF was dried by passage through solvent purification columns containing activated alumina. $CHCl_3$, dichloromethane (DCM), and toluene were high-performance liquid chromatography (HPLC) grade and were used without further purification. All reagents were obtained from commercial sources and used without further purification, unless noted otherwise. Flash column chromatography was performed using silica gel (Merck, No. 9385, 230−400 mesh). ^{1}H and ^{13}C{^{1}H} NMR spectra were recorded at 300, 500, or

700 MHz (^{1}H NMR), at 75 or 125 MHz (^{13}C{^{1}H}NMR) using $CDCl_3$ or deuterated dimethyl sulfoxide (DMSO-d_6) as solvent with the residual solvent signal as internal reference ($CDCl_3$ 7.26 and 77.2 ppm and DMSO-d_6 2.50 and 39.5 ppm). High-resolution mass spectrometry (HRMS) by the electrospray ionization (ESI) technique was performed with an Agilent 6500 accurate mass apparatus with a quadrupole time-of-*fl*ight (Q-TOF) analyzer. IR spectra were recorded on a mid-infrared (MIR) (8000−400 cm^{-1}) spectrometer as solid *fi*lms by slow evaporation of the solvent, using the attenuated total re*fl*ectance (ATR) technique. Cyclic voltammograms were recorded using a Metrohm Autolab Potentiostat model PGSTAT302N with a glassy carbon working electrode, Ag/AgCl 3 M as reference, and a Pt wire counter electrode. All the measurements were performed under Ar, at room temperature, from CH_3CN solutions containing 0.1 M [(n-Bu)$_4$N]ClO_4 as supporting electrolyte, with analyte concentrations of 1 mM (scan rate 0.1 V/s).

Compound 3a was obtained from commercial sources and used without any further puri*fi*cation. *p*-Azidoaniline,[26] 3b,[27] 6-chloro-9-octhylpurine,[28] 6-chloro-9-ethylpurine,[29] 5c,[30] 6-chloro-9-(*β*-D-acetyl-*β*-D-ribofuranosyl)purine,[31] 7,[32] 6-phenyl purine,[33] 11,[34] 13a,[35] 13b,[36] and 13c[37]were prepared by following literature procedures.

Synthesis of 2. A solution of *p*-azidoaniline (1.42 g, 10.58 mmol) in 50 mL of $CHCl_3$ under argon atmosphere was treated with *p*-formaldehyde (477 mg, 15.88 mmol) and heated to 70 °C for 48 h. The reaction mixture was *fi*ltered, and the solvent was evaporated under reduced pressure, a*ff*ording 2 (969 mg, quantitative yield) as a brown solid. ^{1}H NMR (300 MHz, $CDCl_3$) δ 7.01−6.97 (m, 6H, CH_{arom}), 6.93−6.85 (m, 6H, CH_{arom}), 4.82 (s, 6H, CH_2). ^{13}C NMR (75 MHz, $CDCl_3$) δ 145.9 (C), 133.0 (C), 119.9 (CH_{arom}), 119.6 (CH_{arom}), 69.6 (CH_2). IR (*fi*lm): ν_{max} 2923, 2852, 2420, 2094, 1675, 1505, 1388, 1290, 1224, 1159, 1119, 986, 937, 858, 819, cm^{-1}. ESI-HRMS *m/z*: calc. for $C_{21}H_{17}N_{12}$ [M]$^+$ 437.169 37; found 437.170 13.

Synthesis of Azide 1. A degassed solution of $Fe_2S_2(CO)_6$ (784 mg, 2.27 mmol) in 47 mL of anhydrous THF was cooled to −78 °C and treated dropwise with Et_3BHLi (1 M solution in THF) (4.8 mL, 4.76 mmol). Low temperature was maintained while stirring for 15 min before the addition of 2 (1 g, 2.28 mmol) under argon. The mixture was stirred for 5 min before TFA (0.70 mL, 9.08 mmol) was added at −78 °C. The solution was then allowed to reach room temperature, and the solvent was removed under reduced pressure. Flash chromatography over silica gel with hexane/toluene (Hex/Tol) (8:2) yielded azide 1 (640 mg, 56%) as a black solid. ^{1}H NMR (300 MHz, $CDCl_3$) δ 7.00 (d, J = 9.0 Hz, 2H, CH_{arom}), 6.75 (d, J = 9.0 Hz, 2H, CH_{arom}), 4.31 (s, 4H, CH_2). ^{13}C NMR (75 MHz, $CDCl_3$) δ 207.0 (CO), 142.1 (C), 132.3 (C), 120.6 (CH_{arom}), 117.3 (CH_{arom}), 50.0 (CH_2). IR (*fi*lm): ν_{max} 2923, 2853, 2074, 2035, 1996, 1508, 1458 cm^{-1}. ESI-HRMS *m/z*: calc. for $C_{14}H_9Fe_2N_4O_6S_2$ [M + H]$^+$ 504.865 73; found 504.865 12.

General Procedure for the Synthesis of Triazole Derivatives. In an argon-purged *fl*ask, azide 1 (1 equiv) and the corresponding alkyne (1 equiv) were mixed with $CuSO_45H_2O$ (1.2 equiv) and sodium ascorbate (3.0 equiv). The degassed solvent (DMF or THF/water mixture as speci*fi*ed in each case) was added to the mixture of reagents, and the solution was stirred at room temperature until disappearance of the starting materials by thin-layer chromatography (TLC). The solvent was partially removed under vacuum, and the concentrated solution was extracted with $CHCl_3$. The organic layer was washed with brine and dried over $MgSO_4$, and the solvent was removed under reduced pressure. The crude products were puri*fi*ed by column chromatography on silica gel.

Synthesis of 4a. According to the general procedure, azide 1 (200 mg, 0.39 mmol), 4-ethynyltoluene (50.3 *μ*L, 0.39 mmol), $CuSO_4$·$5H_2O$ (118.9 mg, 0.48 mmol), and sodium ascorbate (235.8 mg, 1.19 mmol) were stirred at room temperature for 20 h in 15 mL of degassed DMF. The crude was puri*fi*ed by *fl*ash column chromatography on silica gel, using DCM as eluent, to yield 4a (181.2 mg, 75%) as red solid. ^{1}H NMR (300 MHz, $CDCl_3$) δ 8.09 (s, 1H, $CH_{triazole}$), 7.81 (d, J = 7.9 Hz, 2H, CH_{arom}), 7.75 (d, J = 8.9 Hz, 2H, CH_{arom}), 7.28 (d, J = 7.9 Hz, 2H, CH_{arom}), 6.89 (d, J = 8.9 Hz, 2H, CH_{arom}), 4.38 (s, 4H, CH_2), 2.42 (s, 3H, CH_3). ^{13}C NMR (176 MHz, $CDCl_3$) δ 206.9 (CO), 148.5 (C), 144.8 (C), 138.4 (C), 130.1 (C), 129.7 (CH_{arom}), 125.8 (CH_{arom}), 122.4 (CH_{arom}), 117.2 ($CH_{triazole}$), 116.4 (CH_{arom}), 110.1 (C), 49.8 (CH_2), 21.5 (CH_3). IR (*fi*lm): ν_{max} 2924, 2855, 2111, 2083, 2031, 2000, 1964, 1522, 1383, 1231, 1202, 1038, 917, 816, 613 cm^{-1}. ESI-HRMS *m/z*: calc. for $C_{23}H_{17}Fe_2N_4O_6S_2$ [M + H]$^+$ 620.928 36; found 620.930 31.

Synthesis of 4b. According to the general procedure, azide 1 (100 mg, 0.19 mmol), 2-(4-ethynylphenyl)pyridine 3b (35.5 mg, 0.19 mmol), $CuSO_45H_2O$ (59.3 mg, 0.23 mmol), and sodium ascorbate (117.9, 0.59 mmol) were stirred at room temperature for 24 h in 6 mL of degassed DMF. The crude was puri*fi*ed by *fl*ash column chromatography on silica gel, using DCM/ethyl acetate (AcOEt) (0 to 50%) as eluent, to yield 4b (108 mg, 80%) as a red solid. ^{1}H NMR (700 MHz, $CDCl_3$) δ 8.74 (d, J = 3.8 Hz, 1H, CH_{PhPy}), 8.21 (s, 1H, $CH_{triazole}$), 8.13 (d, J = 8.0 Hz, 2H, CH_{PhPy}), 8.05 (d, J = 8.0 Hz, 2H, CH_{PhPy}), 7.84−7.74 (m, 5H, CH_{arom}), 6.91 (d, J = 8.7 Hz, 2H, CH_{arom}), 4.39 (s, 4H, CH_2). ^{13}C NMR (75 MHz, $CDCl_3$) δ 206.9 (CO), 156.9 (C), 149.9 (CH), 148.0 (C), 144.9 (C), 139.3 (C), 136.9 (CH), 131.0 (C), 129.9 (C), 127.5 (CH), 126.3 (CH), 122.5 (CH), 122.3 (CH), 120.6 (C), 117.9 (CH), 116.4 (CH), 49.8 (CH_2). IR (*fi*lm): ν_{max} 2923, 2853, 2077, 2033, 1994, 1736, 1683, 1610, 1584, 1521, 1464, 1438, 1380, 1260, 1237, 1198, 1099, 1037, 815, 783, 737 cm^{-1}. ESI-HRMS *m/z*: calc. for $C_{27}H_{18}Fe_2N_5O_6S_2$ [M + H]$^+$ 683.939 28; found 683.936 15.

Synthesis of 6a. According to the general procedure, azide 1 (360 mg, 0.71 mmol), 5a (102.2 mg, 0.71 mmol), $CuSO_45H_2O$ (213.9 mg, 0.85 mmol), and sodium ascorbate (424.3, 2.14 mmol) were stirred at room temperature for 24 h in 21 mL of degassed DMF. The crude was puri*fi*ed by *fl*ash column chromatography on silica gel, using DCM/AcOEt (8:2) as eluent, to yield 6a (195.6 mg, 43%) as red solid. ^{1}H NMR (700 MHz, DMSO-d_6) δ 9.51 (s, 1H, CH_{purine}), 9.01 (s, 1H, CH_{purine}), 8.75 (s, 1H, $CH_{triazole}$), 8.00 (d, J = 8.7 Hz, 2H, CH_{arom}), 7.18 (d, J = 8.7 Hz, 2H, CH_{arom}), 4.67 (s, 4H, CH_2), 4.33 (t, J = 7.2 Hz, 2H, CH_2), 1.90 (p, J = 7.2 Hz, 2H, CH_2), 1.39−1.10 (m, 12H, CH_2), 0.83 (t, J = 7.0 Hz, 3H, CH_3). ^{13}C NMR (176 MHz, DMSO-d_6) δ 207.1 (C), 152.1 (C), 152.0 (CH_{purine}), 146.9 (CH_{purine}), 146.15 (C), 144.4 (C), 143.5 (C), 129.3 (C), 128.5 (C), 125.01 ($CH_{triazole}$), 122.09 (CH_{arom}), 116.16 (CH_{arom}), 48.99, 43.30, 31.15, 29.10, 28.53, 28.38, 26.01, 22.06 (all CH_2), 13.9 (CH_3). IR (*fi*lm): ν_{max} 2925, 2855, 2074, 2034, 1995, 1601, 1522, 1455, 1385, 1325, 1268, 1205, 1144, 1036, 917, 823, 646, 615, 582 cm^{-1}. ESI-HRMS *m/z*: calc. for $C_{29}H_{28}Fe_2N_8O_6S_2$ [M + H]$^+$ 761.034 95; found 761.034 59.

Synthesis of 6b. According to the general procedure, azide 1 (100 mg, 0.19 mmol), 5b (49.2 mg, 0.19 mmol), $CuSO_45H_2O$ (59.3 mg, 0.23 mmol), and sodium ascorbate (117.9, 0.59 mmol) were stirred at room temperature for 24 h in 6 mL of degassed DMF. The crude was puri*fi*ed by *fl*ash column chromatography on silica gel, using DCM/AcOEt (8:2) as eluent, to yield 6b (146 mg, 97%) as a red solid. ^{1}H NMR (700 MHz, $CDCl_3$) δ 9.06 (s, 1H, CH_{purine}) 8.94 (d, J = 8.0 Hz, 2H, CH_{arom}), 8.24 (s, 1H, $CH_{triazole}$), 8.18 (s, 1H, CH_{purine}), 8.13 (d, J = 8.0 Hz, 2H, CH_{arom}), 7.77 (d, J = 8.5 Hz, 2H, CH_{arom}), 6.90 (d, J = 8.5 Hz, 2H, CH_{arom}), 4.42 (q, J = 7.3 Hz, 2H, CH_2), 4.39 (s, 4H, CH_2), 1.63 (t, J = 7.3 Hz, 3H, CH_3). ^{13}C NMR (176 MHz, $CDCl_3$) δ 206.9 (CO), 152.6 (C), 152.4 (CH), 145.0 (C), 144.0 (CH), 140.2, 135.8, 132.7, 131.3 (all C), 130.5 (CH), 129.9 (C), 126.1 (CH_{arom}), 123.6 (C), 122.5, 118.2, 116.45 (all CH_{arom}), 49.8 (CH_2), 39.1 (CH_2), 15.6 (CH_3). IR (*fi*lm): ν_{max} 2925, 2073, 2031, 1994, 1611, 1578, 1521, 1504, 1447, 1384, 1325, 1262, 217, 1199, 1039, 916, 862, 757 cm^{-1}. ESI-HRMS *m/z*: calc. *para*-$C_{30}H_{23}Fe_2N_7O_6S_2$ [M + H]$^+$ 752.984 57; found 752.986 40.

Synthesis of 6c. According to the general procedure, azide 1 (100 mg, 0.19 mmol), 5c (79.8 mg, 0.19 mmol), $CuSO_45H_2O$ (59.3 mg, 0.23 mmol), and sodium ascorbate (117.9, 0.59 mmol) were stirred at room temperature for 40 h in 6 mL of degassed DMF. The crude was puri*fi*ed by *fl*ash column chromatography on silica gel, using AcOEt as eluent, to yield 6c (98.0 mg, 55%) as a red solid. ^{1}H NMR (300 MHz, $CDCl_3$) δ 9.13 (s, 1H, CH_{purine}), 9.10 (s, 1H, CH_{purine}), 8.31 (s, 1H, $CH_{triazole}$), 7.84 (d, J = 8.9 Hz, 2H, CH_{arom}), 6.90 (d, J = 8.9 Hz, 1H, CH_{arom}), 6.34−6.29 (m, 1H, CH_{ribose}), 6.05−5.97 (m, 1H, CH_{ribose}),

5.75−5.69 (m, 1H, CH_{ribose}), 4.53−4.43 (m, 3H, CH_{ribose} + $CH_{2\ ribose}$), 4.38 (s, 4H, CH_2), 2.18, 2.15, 2.11 (all s, 3H, all $CH_{3\ AcO}$). ^{13}C NMR (176 MHz, $CDCl_3$) δ 206.9 (CO), 170.4, 169.7, 169.5 (all CO_{AcO}), 153.4 (CH_{purine}), 151.8, 147.9 (both C), 145.2 (CH_{purine}),144.0, 143.2, 130.5, 129.6, 124.7 (all C), 122.8, 116.3 (both CH_{arom}), 86.6, 80.6, 73.3, 70.7 (all CH_{ribose}), 63.1 ($CH_{2\ ribose}$), 49.7 (CH_2), 20.9, 20.7, 20.5 (all $CH_{3\ AcO}$). IR (*fi*lm): ν_{max} 2920, 2852, 2073, 2035, 1997, 1747, 1600, 1553, 1522, 1420, 1372, 1222, 1044, 906, 824 cm^{-1}. ESI-HRMS *m/z*: calc. for $C_{29}H_{21}Fe_2N_8O_6S_2$ [M + H]$^+$ 752.971 99; found 752.972 47.

Synthesis of 6d. According to the general procedure, azide 1 (100 mg, 0.19 mmol), 5d (94.7 mg, 0.19 mmol), $CuSO_4 5H_2O$ (59.3 mg, 0.23 mmol), and sodium ascorbate (117.9, 0.59 mmol) were stirred at room temperature for 24 h in 6 mL of degassed DMF. The crude was puri*fi*ed by *fl*ash column chromatography on silica gel, using AcOEt as eluent, to yield 6d (165.4 mg, 85%) as red solid. ^{1}H NMR (300 MHz, $CDCl_3$) δ 9.06 (s, 1H, CH_{purine}), 8.92 (d, *J* = 8.2 Hz, 2H, CH_{arom}), 8.31 (s, 1H, CH_{purine}), 8.24 (s, 1H, $CH_{triazole}$), 8.13 (d, *J* = 8.2 Hz, 2H, CH_{arom}), 7.77 (d, *J* = 8.9 Hz, 2H, CH_{arom}), 6.90 (d, *J* = 8.9 Hz, 2H, CH_{arom}), 6.32 (d, *J* = 5.3 Hz, 1H, CH_{ribose}), 6.03 (t, *J* = 5.3 Hz, 1H, CH_{ribose}), 5.72 (t, *J* = 5.2 Hz, 1H, CH_{ribose}), 4.53−4.41 (m, 3H, CH_{ribose} + $CH_{2\ ribose}$), 4.38 (s, 4H, CH_2), 2.18, 2.16, 2.10 (all s, 9H, $CH_{3\ AcO}$). ^{13}C NMR (176 MHz, $CDCl_3$) δ 206.9 (CO), 170.4, 169.7, 169.5 (all CO_{AcO}), 154.8 (C), 152.8 (CH), 152.2, 147.8, 145.0 (C), 142.7 (CH), 139.4, 135.4, 133.0, 131.8, (C), 130.6 (CH_{arom}), 130.0, 129.9, 128.6 (C), 126.1 (CH_{arom}), 122.5 (CH_{arom}), 118.3 (CH), 116.4 (CH_{arom}), 86.5, 80.5, 73.2, 70.8 (all CH_{ribose}), 63.2 ($CH_{2\ ribose}$), 49.8 (CH_2), 20.9, 20.7, 20.6 (all $CH_{3\ AcO}$). IR (*fi*lm): ν_{max} 2920, 2074, 2034, 1996, 1749, 1580, 1521, 1446, 1375, 1327, 1221, 1099, 1041, 918, 860, 802, 615 cm^{-1}. ESI- HRMS *m/z*: calc. for $C_{38}H_{31}Fe_2N_8O_{13}S_2$ [M + H]$^+$ 983.014 72; found 983.016 85.

Synthesis of 8. According to the general procedure, azide 1 (50 mg, 0.09 mmol), 7 (46.9 mg, 0.09 mmol), $CuSO_4 5H_2O$ (29.7 mg, 0.12 mmol), and sodium ascorbate (58.9, 0.29 mmol) were stirred at room temperature for 30 h in 3 mL of degassed DMF. The crude was puri*fi*ed by *fl*ash column chromatography on silica gel, using DCM/AcOEt (8:2) as eluent, to yield 8 (70.5 mg, 78%) as a red solid. ^{1}H NMR (300 MHz, DMSO-d_6) δ 11.91 (s, 1H, OH_{major}), 8.81 (s, 1H, $CH_{triazole}$), 8.50 (s, 1H, $CH_{pyrimidine}$), 8.31 (s, 1H, NH_{minor}), 7.88 (d, *J* = 8.6 Hz, 2H, CH_{arom}), 7.13 (d, *J* = 8.8 Hz, 2H, CH_{arom}), 6.11 (d, *J* = 5.3 Hz, 1H, CH_{ribose}), 5.53 (t, *J* = 5.7 Hz, 1H, CH_{ribose}), 5.41 (t, *J* = 5.3 Hz, 1H, CH_{ribose}), 4.64 (s, 4H, CH_2), 4.50−4.03 (m, 3H, $CH_{2\ ribose}$ + CH_{ribose}), 2.16, 2.11, 2.07 (all s, 3H, CH_3). ^{13}C NMR (176 MHz, DMSO) δ 207.1 (CO), 170.1 (C), 169.3(C), 160.9 (C), 149.5 (C), 144.0 (C), 139.3 (C), 136.8 (CH), 128.7 (C), 121.7 (CH), 120.0 (CH), 116.0 (CH), 105.5 (C), 87.8, 79.4, 79.1, 72.2, 69.9 (all CH), 63.0 (CH_2), 48.9 (CH_2), 20.5, 20.3, 20.2 (all CH_3). IR (*fi*lm): ν_{max} 3079, 2926, 2074, 2035, 1996, 1748, 1715, 1521, 1465, 1375, 1230, 1100, 1041, 914, 818, 730, 613, 581 cm^{-1}. ESI-HRMS *m/z*: calc. For $C_{31}H_{27}Fe_2N_6O_{15}S_2$ [M + H]$^+$ 898.967 06; found 898.971 31.

Synthesis of 10. According to the general procedure, azide 1 (100 mg, 0.19 mmol), 9 (49.1 mg, 0.19 mmol), $CuSO_4 5H_2O$ (59.3 mg, 0.23 mmol), and sodium ascorbate (117.9, 0.59 mmol) were stirred at room temperature for 20 h in 6 mL of degassed DMF. The crude was puri*fi*ed by *fl*ash column chromatography on silica gel, using DCM/AcOEt (8:2) as eluent, to yield 10 (49.1 mg, 82%) as red solid. ^{1}H NMR (500 MHz, $CDCl_3$) δ 9.04 (s, 1H, CH_{purine}), 8.76 (d, *J* = 6.8 Hz, 2H, CH_{Ph}), 8.05 (s, 1H, $CH_{triazole}$), 7.77−7.42 (m, 6H, CH_{Ph} + CH_{purine} + CH_{arom}), 6.80 (d, *J* = 9.1 Hz, 2H, CH_{arom}), 4.81 (t, *J* = 6.7 Hz, 2H, CH_2), 4.32 (s, 4H, CH_2), 3.45 (t, *J* = 6.7 Hz, 2H, CH_2). ^{13}C NMR (126 MHz, $CDCl_3$) δ 206.8 (CO), 155.0, 152.5 (both C), 152.4 (CH), 145.0 (C), 144.9 (CH), 143.8, 135.7, 131.2 (all C), 131.1 (CH), 129.9 (C), 129.7 (CH), 128.8 (CH), 122.4 (CH), 120.3 (CH), 116.3 (CH), 49.7, 43.3, 26.2 (all CH_2). IR (*fi*lm): ν_{max} 2921, 2852, 2073, 2035, 1996, 1741, 1572, 1521, 1452, 1377, 1325, 1261, 1208, 1094, 1048, 818, 767, 696, 643, 619 cm^{-1}. ESI-HRMS *m/z*: calc. for $C_{29}H_{21}Fe_2N_8O_6S_2$ [M + H]$^+$ 752.971 99; found 752.972 47.

Synthesis of 12. According to the general procedure, azide 1 (100 mg, 0.19 mmol, 1equiv), alkyne 11 (68.9 mg, 0.19 mmol), $CuSO_4 5H_2O$ (59.3 mg, 0.23 mmol), and sodium ascorbate (117.9, 0.59 mmol) were stirred at room temperature for 48 h in 6 mL of degassed THF and 6 mL of degassed water. The crude was puri*fi*ed by *fl*ash column chromatography on silica gel, using DCM/AcOEt (1:1) as eluent, to yield 12 (65 mg, 39%) as dark pink solid. ^{1}H NMR (300 MHz, $CDCl_3$) δ 8.23 (s, 1H, $CH_{triazole}$), 8.08 (d, *J* = 8.0 Hz, 2H, CH_{arom}), 7.77 (d, *J* = 7.8 Hz, 2H, CH_{arom}), 7.41 (d, *J* = 7.8 Hz, 2H, CH_{arom}), 6.91 (d, *J* = 8.0 Hz, 2H, CH_{arom}), 6.01 (s, 2H, CH_{arom}), 4.39 (s, 4H, CH_2), 2.58 (s, 6H, CH_3), 1.47 (s, 6H, CH_3). ^{13}C NMR (176 MHz, $CDCl_3$) δ 206.8 (CO), 155.7 (C), 147.6 (C), 144.9 (C), 143.2 (C), 141.2 (C), 135.1 (C), 131.4 (C), 131.1 (C), 129.8 (C), 128.8 (CH_{arom}), 126.6 (CH_{arom}), 122.5 (CH_{arom}), 121.4 (CH_{arom}), 118.1 ($CH_{triazole}$), 116.4 (CH_{arom}), 49.7 (CH_2), 14.8 (CH_3). IR (*fi*lm): ν_{max} 2923, 2853, 2074, 2035, 1997, 1609, 1544, 1514, 1468, 1195, 1158, 1083, 1046, 981 cm^{-1}. ESI- HRMS *m/z*: calc. for $C_{35}H_{28}BF_2Fe_2N_6O_6S_2$ [M + H]$^+$ 853.027 41; found 853.027 49.

Synthesis of 14a. According to the general procedure, azide 1 (100 mg, 0.19 mmol), ethynylferrocene (41.5 mg, 0.19 mmol), $CuSO_4 \cdot 5H_2O$ (59.3 mg, 0.23 mmol), and sodium ascorbate (117.9, 0.59 mmol) were stirred at room temperature for 48 h in a mixture of 6 mL of degassed THF and 6 mL of degassed water. The crude was puri*fi*ed by *fl*ash column chromatography on silica gel using DCM/AcOEt (0% to 50%) as eluent, to yield 14a (102 mg, 72%) as reddish-brown solid. ^{1}H NMR (300 MHz, $CDCl_3$) δ 7.82 (s, 1H, $CH_{triazole}$), 7.74 (d, *J* = 8.9 Hz, 2H, CH_{arom}),6.89 (d, *J* = 9.0 Hz, 2H, CH_{arom}), 4.79 (s, 2H, CH_{Cp}), 4.38 (s, 4H, CH_2), 4.35 (s, 2H, CH_{Cp}), 4.14 (s, 5H, CH_{Cp}). ^{13}C NMR (176 MHz, $CDCl_3$) δ 206.9 (C), 147.5 (C), 144.8 (C), 130.1 (C), 122.2 (CH_{arom}), 116.6 ($CH_{triazole}$), 116.4 (CH_{arom}), 69.76 (CH_{Cp}), 68.9 (CH_{Cp}), 66.9 (CH_{Cp}), 49.8 (CH_2). IR (*fi*lm): ν_{max} 2922, 2850, 2079, 2036, 1980, 1521, 1384, 1261, 1200, 1045, 816 cm^{-1}. ESI-HRMS *m/z*: calc. for $C_{26}H_{19}Fe_3N_4O_6S_2$ [M + H]$^+$ 714.879 03; found 714.878 14.

Synthesis of 14b. According to the general procedure, azide 1 (100 mg, 0.19 mmol), ethynylruthenocene (50.6 mg, 0.19 mmol), $CuSO_4 \cdot 5H_2O$ (59.3 mg, 0.23 mmol), and sodium ascorbate (117.9, 0.59 mmol) were stirred at room temperature for 20 h in 15 mL of degassed DMF. The crude was puri*fi*ed by *fl*ash column chromatography on silica gel, using DCM as eluent to yield 14b (120.0 mg, 79%) as a red solid. ^{1}H NMR (700 MHz, $CDCl_3$) δ 7.74 (s, 1H, $CH_{triazole}$), 7.69 (d, *J* = 8.5 Hz, 2H, CH_{arom}), 6.87 (d, *J* = 8.5 Hz, 2H, CH_{arom}), 5.19 (s, 2H, Cp), 4.70 (s, 2H, Cp), 4.54 (s, 5H, Cp), 4.37 (s, 4H, CH_2). ^{13}C NMR (75 MHz, $CDCl_3$) δ 206.9 (CO), 145.7 (C), 144.5 (C), 129.7 (C), 122.2 (CH_{arom}), 116.9 ($CH_{triazole}$), 116.3 (CH_{arom}), 78.9 (C_{Cp}), 71.6 (CH_{Cp}), 70.82 (CH_{Cp}), 69.5 (CH_{Cp}), 49.8 (CH_2). IR (*fi*lm): ν_{max} 2923, 2855, 2078, 2039, 1986, 1521, 1451, 1385, 1201, 1045, 918, 811 cm^{-1}. ESI-HRMS *m/z*: calc. for $C_{26}H_{19}Fe_2N_4O_6RuS_2$ [M + H]$^+$ 760.849 25; found 760.847 65.

Synthesis of 14c. According to the general procedure, azide 1 (100 mg, 0.19 mmol), ethynylcymantrene (57.1 mg, 0.19 mmol), $CuSO_4 \cdot 5H_2O$ (59.3 mg, 0.23 mmol), and sodium ascorbate (117.9, 0.59 mmol) were stirred at room temperature for 48 h in a mixture of 6 mL of degassed THF and 6 mL of degassed water. The crude was puri*fi*ed by *fl*ash column chromatography on silica gel, using DCM/AcOEt (0% to 50%) as eluent, to yield 14c (95 mg, 65%) as a reddish-brown solid. ^{1}H NMR (300 MHz, $CDCl_3$) δ 7.90 (s, 1H, $CH_{triazole}$), 7.70 (d, *J* = 9.6 Hz, 2H, CH_{arom}), 6.88 (d, *J* = 9.6 Hz, 2H, CH_{arom}), 5.39 (s, 2H, CH_{Cp}), 4.85 (s, 2H, CH_{Cp}), 4.37 (s, 4H, CH_2). ^{13}C NMR (176 MHz, $CDCl_3$) δ 224.6 (CO_{Mn}), 206.9 (CO_{Fe}), 184.3 (C), 145.1 (C), 129.64, 122.6 (CH_{arom}), 118.0 ($CH_{triazole}$), 116.3 (CH_{arom}), 92.4 (C),82.3 (CH_{Cp}), 81.7 (CH_{Cp}), 49.8 (CH_2). IR (*fi*lm): ν_{max} 2075, 2027, 1997, 1929, 1609, 1521, 1455, 1384, 1270, 1202, 1043, 916, 820, 665, 632, 581 cm^{-1}. ESI- HRMS *m/z*: calc. for $C_{24}H_{14}Fe_2MnN_4O_9S_2$ [M + H]$^+$ 732.827 69; found 732.829 24.

Synthesis of 16. According to the general procedure, azide 1 (51.7 mg, 0.10 mmol), 15 (50.0 mg, 0.10 mmol), $CuSO_4 5H_2O$ (30.7 mg, 0.12 mmol), and sodium ascorbate (61.0, 0.31 mmol) were stirred at room temperature for 30 h in 3 mL of degassed DMF. The crude was *fi*ltered, and the red solid was washed with water and Et_2O and dried in vacuum, to yield 16 (85.0 mg, 83%) as a red solid. ^{1}H NMR (700 MHz, DMSO-d_6) δ 9.11 (s, 1H, $CH_{triazole}$), 7.90−7.84 (m, 4H,

CH_{arom}), 7.17 (d, J = 8.1 Hz, 2H, CH_{arom}), 7.06 (d, J = 7.9 Hz, 2H, CH_{arom}), 5.10−4.44 (m, 8H, CH_2). ^{13}C NMR (176 MHz, DMSO-d_6) δ 207.2 (CO), 147.0 (C), 143.9 (C), 143.6 (C), 129.0 (C), 126.7 (C), 126.3 (CH), 121.3 (CH), 118.0 (CH), 117.8 (C), 116.1 (CH), 115.7 (CH), 48.9 (CH_2). IR (film): ν_{max} 2923, 2855, 2077, 2030, 1984, 1956, 1609, 1517, 1494, 1451, 1380, 1258, 1229, 1193, 1140, 1032, 1005, 911, 876, 811, 779, 667, 611, 564 cm^{-1}. ESI-HRMS m/z: calc. For $C_{30}H_{18}Fe_4N_5O_{12}S_4$ [M + H]$^+$ 991.7230; found 991.726 80.

Synthesis of Me4a$^+$. In a flame-dried flask a mixture of 4a (80 mg, 0.12 mmol) and trimethyloxonium tetrafluoroborate (28.0 mg, 0.19 mmol) was dissolved with 8.5 mL of dry DCM. The mixture was stirred at room temperature for 72 h. After the solvent was removed under reduced pressure, the crude was purified by flash column chromatography on silica gel using DCM to DCM/AcOEt/MeOH (9:1:1) as eluent to yield Me4a$^+$ (56.4 mg, 60%). ^1H NMR (300 MHz, acetone-d_6) δ 9.47 (s, 1H, $CH_{triazol}$), 8.07 (d, J = 9.2 Hz, 2H, CH_{arom}), 7.79 (d, J = 7.9 Hz, 2H, CH_{arom}), 7.55 (d, J = 7.9 Hz, 2H, CH_{arom}), 7.40−7.26 (d, J = 9.2 Hz, 2H, CH_{arom}), 4.69 (s, 4H, CH_2), 4.58 (s, 3H, NCH_3), 2.48 (s, 3H, CH_3). ^{13}C NMR (75 MHz, acetone-d_6) δ 208.2 (CO), 145.1 (C), 143.39 (C), 131.1 (CH_{arom}), 130.3 (CH_{arom}), 127.8 (CH), 126.8 ($CH_{triazol}$), 123.9 (CH_{arom}), 120.8 (C), 117.2 (CH_{arom}), 115.2 (CH_{arom}), 50.0 (CH_2), 39.6 (NCH_3), 21.5 (CH_3). IR (film): ν_{max} 3675, 3658, 3601, 3492, 2954, 2924, 2852, 2074, 2034, 1996, 1706, 1605, 1520, 1505, 1446, 1363, 1282, 1261, 1221, 1059, 915, 820, 614, 579, 562 cm^{-1}. ESI-HRMS m/z: calc. For $C_{24}H_{21}Fe_2N_4O_6S_2$ [M]$^+$ 634.944 02; found 634.945 56.

ASSOCIATED CONTENT

Supporting Information

The Supporting Information is available free of charge on the ACS Publications website at DOI: 10.1021/acs.inorgchem.9b02813.

Full experimental details for the preparation of compounds 5a, 5b, 5d, 9, and 15, spectroscopic data for the compounds reported, as well as electrochemical studies indicated in the text (PDF)

Accession Codes

CCDC 1884096−1884097 contain the supplementary crystallographic data for this paper. These data can be obtained free of charge via www.ccdc.cam.ac.uk/data_request/cif, or by emailing data_request@ccdc.cam.ac.uk, or by contacting The Cambridge Crystallographic Data Centre, 12 Union Road, Cambridge CB2 1EZ, UK; fax: +44 1223 336033.

AUTHOR INFORMATION

Corresponding Author

*E-mail: sierraor@ucm.es.

ORCID

Alba Collado: 0000-0001-6215-1822

Luis Casarrubios: 0000-0002-9054-3118

Mar Gómez-Gallego: 0000-0002-8961-7685

Antonio Caballero: 0000-0002-8229-6866

Fabiola Zapata: 0000-0002-7474-2280

Miguel A. Sierra: 0000-0002-3360-7795

Notes

The authors declare no competing financial interest.

ACKNOWLEDGMENTS

Support for this work under Grant Nos. CTQ2016-77555-C2-1-R and CTQ2016-81797-REDC (Programa Redes Consolider) from the MINECO (Spain) and from Fundación Ramón Areces (CIVP18A3938) is gratefully acknowledged. A.C. thanks the MINECO for her Juan de la Cierva-Incorporación fellowship. A.D.M. thanks MINECO for an FPI grant. We also thank the SCSIE-UV for X-ray facilities.

REFERENCES

(1) (a) Lubitz, W.; Ogata, H.; Rüdiger, O.; Reijerse, W. Hydrogenases. *Chem. Rev.* 2014, *114*, 4081−4148. (b) Vignais, P. M.; Billoud, B. Occurrence, Classification and Biological Function of Hydrogenases: An Overview. *Chem. Rev.* 2007, *107*, 4206−4272.

(2) (a) *Hydrogen as a Fuel: Learning from Nature,;* Cammack, R., Frey, M., Robson, R., Eds.; Taylor&Francis, 2001. (b) *Compendium of Hydrogen Energy Vol. 1: Hydrogen Production and Purification;* Subramani, V., Basile, A., Veziroğlu, T. N., Eds.; Elsevier, 2015. (c) Dincer, I.; Zamfirescu, C. *Sustainable Hydrogen Production;* Elsevier, 2016. (d) *Compendium of Hydrogen Energy Vol. 4: Hydrogen Use, Safety and the Hydrogen Economy;* Ball, M., Basile, A., Veziroğlu, T. N., Eds.; Elsevier, 2016.

(3) See, for example: (a) Reisner, E.; Powell, D. J.; Cavazza, C.; Fontecilla-Camps, J. C.; Armstrong, F. A. Visible Light-Driven H_2 Production by Hydrogenases Attached to Dye-Sensitized TiO_2 Nanoparticles. *J. Am. Chem. Soc.* 2009, *131*, 18457−18466. (b) Brown, K. A.; Dayal, S.; Ai, X.; Rumbles, G.; King, P. W. Controlled Assembly of Hydrogenase-CdTe Nanocrystal hybrids for Solar Hydrogen Production. *J. Am. Chem. Soc.* 2010, *132*, 9672−9680. (c) Brown, K. A.; Wilker, B.; Boehm, M.; Dukovic, G.; King, P. W. Characterization of Photochemical Processes for H_2 Production by CdS Nanorod-[Fe-Fe] Hydrogenase Complexes. *J. Am. Chem. Soc.* 2012, *134*, 5627−5636. (d) Honda, Y.; Hagiwara, H.; Ida, S.; Ishihara, T. Application to Photocatalytic H_2 Production of a Whole-Cell Reaction by Recombinant Escherichia coli Cells Expressing [Fe-Fe]-Hydrogenase and Maturases Genes. *Angew. Chem., Int. Ed.* 2016, *55*, 8045−8048.

(4) Representative examples: (a) Li, H.; Rauchfuss, T. B. Iron Carbonyl Sulfides, Formaldehyde and Amines Condense to Give the proposed Azadithiolate Cofactor of the Fe-Only Hydrogenases. *J. Am. Chem. Soc.* 2002, *124*, 726−727. (b) Na, Y.; Pan, J.; Wang, M.; Sun, L. Intermolecular Electron Transfer from Photogenerated $Ru(bpy)^{3+}$ to [2Fe2S] Model Complexes of the Iron-Only Hydrogenase Active Site. *Inorg. Chem.* 2007, *46*, 3813−3815. (c) Gao, S.; Fan, J.; Sun, S.; Peng, X.; Zhao, X.; Hou, J. Selenium-Bridged Diiron Hexacarbonyl Complexes as Biomimetic Models for the Active Site of Fe-Fe Hydrogenases. *Dalton Trans.* 2008, 2128−2135. (d) Li, P.; Wang, M.; Chen, L.; Liu, J.; Zhao, Z.; Sun, L. Structures, Protonation and Electrochemical Properties of Diiron Dithiolate Complexes Containing Pyridyl-Phosphine Ligands. *Dalton Trans.* 2009, 1919−1926. (e) Apfel, U.-P.; Troegel, D.; Halpin, Y.; Tschierlei, S.; Uhlemann, U.; Görls, H.; Schmitt, M.; Popp, J.; Dunne, P.; Venkatesan, M.; Coey, M.; Rudolph, M.; Vos, J. G.; Tacke, R.; Weigand, W. Models for the Active Site in [FeFe] Hydrogenase with Iron-Bound Ligands Derived from Bis-, Tris-, and Tetrakis(mercaptomethyl)silanes. *Inorg. Chem.* 2010, *49*, 10117−10132. (f) Camara, J. M.; Rauchfuss, T. B. Combining Acid-Base, Redox and Substrate Binding Functionalities to Give a Complete Model for the [FeFe]-Hydrogenase. *Nat. Chem.* 2012, *4*, 26−30. (g) Zheng, D.; Wang, M.; Chen, L.; Wang, N.; Sun, L. Redox Reactions of [FeFe]-Hydrogenase Models Containing an Internal Amine and a Pendant Phosphine. *Inorg. Chem.* 2014, *53*, 1555−1561. (h) Yu, T.; Zeng, Y.; Chen, J.; Li, Y.-Y.; Yang, G.; Li, Y. Exceptional Dendrimer-Based Mimics of Diiron Hydrogenase for the Photochemical Production of Hydrogen. *Angew. Chem., Int. Ed.* 2013, *52*, 5631−5635 Revisions: . (i) Schilter, m L.; Camara, J. M.; Huynh, M. T.; Hammes-Schiffer, S.; Rauchfuss, T. B. Hydrogenase Enzymes and Their Synthetic Models: The Role of Metal Hydrides. *Chem. Rev.* 2016, *116*, 8693−8749. (j) Li, Y.; Rauchfuss, T. B. Synthesis of Diiron(I) Dithiolato Carbonyl Complexes. *Chem. Rev.* 2016, *116*, 7043−7077.

(5) Samuel, A. P. S.; Co, D. T.; Stern, C. L.; Wasielewski, M. R. Ultrafast Photodriven Intramolecular Electron Transfer from a Zinc Porphyrin to a Readily Reduced Diiron Hydrogenase Model. *J. Am. Chem. Soc.* 2010, *132*, 8813−8815.

(6) Kluwer, A. M.; Kapre, R.; Hartl, F.; Lutz, M.; Spek, A. L.; Brouwer, A. M.; van Leeuwen, P. W. N. M.; Reek, J. N. H. Self-Assembled biomimetic [2Fe2S]-Hydrogenase-based Photocatalyst for molecular Hydrogen Evolution. *Proc. Natl. Acad. Sci. U. S. A.* 2009, *106*, 10460−10465.

(7) Goy, R.; Apfel, U.-P.; Elleouet, C.; Escudero, D.; Elstner, M.; Görls, H.; Talarmin, J.; Schollhammer, P.; González, L.; Weigand, W. A Silicon-Heteroaromatic System as Photosensitizer for Light-Driven Hydrogen Production by Hydrogenase Mimics. *Eur. J. Inorg. Chem.* 2013, *2013*, 4466−4472.

(8) (a) Tornøe, C. W.; Christensen, C.; Meldal, M. Peptidotriazoles on Solid Phase: [1,2,3]-Triazoles by Regiospecific Copper(I)-Catalyzed 1,3-Dipolar Cycloadditions of Terminal Alkynes to Azides. *J. Org. Chem.* 2002, *67*, 3057. (b) Rostovtsev, V. V.; Green, L. G.; Fokin, V. V.; Sharpless, K. B. A Stepwise Huisgen Cycloaddition Process: Copper(I)-Catalyzed Regioselective Ligation of Azides and Terminal Alkynes. *Angew. Chem., Int. Ed.* 2002, *41*, 2596−2599 For selected reviews on the copper(I)-catalyzed azide−alkyne reaction, see: . (c) Meldal, M.; Tornøe, C. W. Cu-Catalyzed Azide-Alkyne Cycloaddition. *Chem. Rev.* 2008, *108*, 2952−3015. (d) Bock, V. D.; Hiemstra, H.; van Maarseveen, J. H. Cu(I)-Catalyzed Alkyne-Azide Click Cycloadditions from a Mechanistic and Synthetic Perspective. *Eur. J. Org. Chem.* 2006, *2006*, 51−68. (e) Binder, W. H.; Sachsenhofer, R. Click Chemistry in Polymer and Materials Science. *Macromol. Rapid Commun.* 2007, *28*, 15−54. (f) Nandivada, H.; Jiang, X.; Lahann, J. Click Chemistry: Versatility and Control in the Hands of Materials Scientists. *Adv. Mater.* 2007, *19*, 2197−2208.

(9) Some selected examples from these laboratories: (a) Pellico, D.; Góez-Gallego, M.; Ramírez-López, P.; Mancheño, M. J.; Sierra, M. A.; Torres, M. R. The Sequential Building of Chiral Macrocyclic Bis-*β*-Lactams by Double Staudinger-Cu-Catalyzed Azide-Alkyne Cycloaddtions. *Chem. - Eur. J.* 2010, *16*, 1592−1600. (b) Montenegro, H. E.; Ramírez-López, P.; de la Torre, M. C.; Asenjo, M.; Sierra, M. A. Two Versatile and Parallel Approaches to Highly Symmetrical Open and Closed Natural Product-Based Structures. *Chem. - Eur. J.* 2010, *16*, 3798−3814. (c) de la Torre, M. C.; Asenjo, M.; Ramírez-López, P.; Sierra, M. A. The Reversible Nicholas Reaction in the Synthesis of Highly Symmetric Natural-Product-Based Macrocycles. *Eur. J. Org. Chem.* 2015, *2015*, 1054−1067. (d) Frutos, M.; de la Torre, M. C.; Sierra, M. A. Steroid Derived Mesoionic Gold and Silver Mono- and Polymetallic Carbenes. *Inorg. Chem.* 2015, *54*, 11174−11185. (e) Frutos, M.; Góez-Gallego, M.; Giner, E. A.; Sierra, M. A.; Ramírez de Arellano, C. Triazole vs. Triazolium Carbene Ligands in the Site-Selective Cyclometallation of *o*-Carboranes by M(III) (M= Ir, Rh) Complexes. *Dalton* 2018, *47*, 9975−9979.

(10) The inverse situation, namely, the CuAAC between an azide and an alkynylphenyl[FeFe] moiety, has been used to anchor the [FeFe]-motif to graphite surfaces. See: Ahmed, M. E.; Dey, S.; Mondal, B.; Dey, A. H2 Evolution Catalyzed by a FeFe-Hydrogenase Synthetic Model Covalently Attached to Graphite Surfaces. *Chem. Commun.* 2017, *53*, 8188−8191.

(11) For a revision of metalla-nucleobases see: Collado, A.; Góez-Gallego, M.; Sierra, M. A. Nucleobases Having M-C Bonds: An Emerging Bio-Organometallic Field. *Eur. J. Org. Chem.* 2018, *2018*, 1617−1623.

(12) Ninety-one structures found in CSD-5.4 Nov 2018 Groom, C. R.; Bruno, I. J.; Lightfoot, M. P.; Ward, S. C. The Cambridge Structural Database. *Acta Crystallogr., Sect. B: Struct. Sci., Cryst. Eng. Mater.* 2016, *B72*, 171−179.

(13) (a) Nicolet, Y.; de Lacey, A. L.; Vernéde, X.; Fernandez, V. M.; Hatchikian, E. C.; Fontecilla-Camps, J. C. Crystallographic and FTIR Spectroscopic Evidence of Changes in Fe Coordination Upon Reduction of the Active Site of the Fe-Only Hydrogenase from Desulfovibrio desulfuricans. *J. Am. Chem. Soc.* 2001, *123*, 1596−1601. (b) Peters, J. W.; Lanzilotta, W. N.; Lemon, B. J.; Seefeldt, L. C. X-ray Structure of the Fe-only Hydrogenase (CpI) from Clostridium Pasteurianum to 1.8 Angstrom Resolution. *Science* 1998, *282*, 1853−1858.

(14) Liu, T.; Wang, M.; Shi, Z.; Cui, H.; Dong, W.; Chen, J.; Åkermark, B.; Sun, L. Synthesis, Structures and Electrochemical Properties of Nitro- and Amino- Functionalized Diiron Azadithiolates as Active Site Models of Fe-Only Hydrogenases. *Chem. - Eur. J.* 2004, *10*, 4474−4479.

(15) A search in the CSD shows that, of the 46 di*ff*erent *N*-arene-substituted hexacarbonyl azadithiolates diirion structures deposited, 45 of them present the arene group in an axial positon of the metallacycle. For these structures the distance range between the C*ipso* and the closest carbonyl group C atom is 3.06−3.30 Å. Furthermore, only one structure presents the *N*-arene group in an equatorial position with a much longer C*ipso*-CO distance (3.496 Å) and corresponds to a 4-aminohepta*f*luorotoluene group; see: Wang, W.-G.; Wang, H.-Y.; Si, G.; Tung, C.-H.; Wu, L.-Z. Fluorophenyl-substituted Fe-Only Hydrogenases active Site adt-Models: Different Electrocatalytic Process for Proton Reduction in HOAc and HBF_4/Et_2O. *Dalton Trans.* 2009, 2712−2720.

(16) (a) Hocek, M.; Fojta, M. Nucleobase Modification as Redox DNA Labelling for Electrochemical Detection. *Chem. Soc. Rev.* 2011, *40*, 5802−5814. (b) Palecek, E.; Bartosik, M. Electrochemistry of Nucleic Acids. *Chem. Rev.* 2012, *112*, 3427−3481.

(17) De Bont, R.; van Larebeke, N. Endogenous DNA Damage in Humans: A Review on Quantitative Data. *Mutagenesis* 2004, *19*, 169.

(18) Cadet, J.; Davies, J. A. Oxidative DNA Damage and Repair: An Introduction. *Free Radical Biol. Med.* 2017, *107*, 2−12. See also the articles in the special issue 107 devoted to *Oxidatively Damaged DNA and its Repair* dedicated to Prof. Tomas Lindahl.

(19) Selected recent reviews: (a) Ulrich, G.; Ziessel, R.; Harriman, A. The Chemistry of Fluorescent Bodipy Dies: Versatility Unsurpassed. *Angew. Chem., Int. Ed.* 2008, *47*, 1184−1201. (b) Boens, N.; Leen, V.; Dehaen, W. Fluorescent Indicators Based on BODIPY. *Chem. Soc. Rev.* 2012, *41*, 1130−1172. (c) Kamkaew, A.; Lim, S. H.; Lee, H. B.; Kiew, L. V.; Chung, L. Y.; Burgess, K. BODIPY Dyes in Photodynamic Therapy. *Chem. Soc. Rev.* 2013, *42*, 77−88. (d) Singh, S. P.; Gayathri, T. Evolution of BODIPY Dyes as Potential Sensitizers for Dye-Sensitized Solar Cells. *Eur. J. Org. Chem.* 2014, *2014*, 4689−4707. (e) Frath, D.; Massue, J.; Ulrich, G.; Ziessel, R. Luminescent Materials: Locking *π*-Conjugated and Heterocyclic Ligands with Boron(III). *Angew. Chem., Int. Ed.* 2014, *53*, 2290−2310. (f) Boens, N.; Verbelen, B.; Dehaen, W. Postfunctionalization of the BODIPY Core: Synthesis and Spectroscopy. *Eur. J. Org. Chem.* 2015, *2015*, 6577−6595.

(20) (a) Capon, J. F.; Gloaguen, F.; Schollhammer, P.; Talarmin, J. Catalysis of the Electrochemicals H_2 evolution by Di-Iron Sub-Site Models. *Coord. Chem. Rev.* 2005, *249*, 1664−1676. (b) Eilers, G.; Schwartz, L.; Stein, M.; Zampella, G.; de Gioia, L.; Ott, S.; Lomoth, R. Ligand versus Metal Protonation of an Iron Hydrogenase Active Site Mimic. *Chem. - Eur. J.* 2007, *13*, 7075−7084. (c) Barton, B. E.; Rauchfuss, T. B. Terminal Hydride in [FeFe]-Hydrogenase Model Has Lower Potential for H_2 Production Than the Isomeric Bridging Hydride. *Inorg. Chem.* 2008, *47*, 2261−2263. (d) Xiao, Z.; Wei, Z.; Long, L.; Wang, Y.; Evans, D. J.; Liu, X. Diiron Carbonyl Complexes Possessing a Fe(II)Fe(II) Core: Synthesis, Characterisation and electrochemical Investigation. *Dalton Trans.* 2011, *40*, 4291−4299. (e) Schilter, D.; Rauchfuss, T. B. And The Winner is- Azadithiolate: An Amine Proton Relay in the [FeFe] Hydrogenases. *Angew. Chem., Int. Ed.* 2013, *52*, 13518−13520. (f) Dey, S.; Rana, A.; Dey, S. G.; Dey, A. Electrochemical Hydrogen Production in Acidc Water by an Azadithiolate Bridged Synthetic Hydrogenase Mimic: Role of Aqueous Solvation in Lowering Overpotential. *ACS Catal.* 2013, *3*, 429−436. (g) Rana, A.; Kumar Das, P.; Mondal, B.; Dey, S.; Crouthers, D.; Dey, A. Investigation of Bridgehead Effects on Reduction Potential in Alkyl and Aryl Azadithiolate-Bridged (μ-SCH_2XCH_2S) $[Fe(CO)_3]_2$ Synthetic Analogues of [FeFe]-H_2ase Active Site. *Eur. J. Inorg. Chem.* 2018, *2018*, 3633−3643.

(21) (a) Gloaguen, F.; Lawrence, J. D.; Schmidt, M.; Wilson, S. R.; Rauchfuss, T. B. Synthetic and Structural Studies on $[Fe_2(SR)_2(CN)_x(CO)_{6-x}]^{x-}$ as Active Site Models for Fe-Only Hydrogenases. *J. Am. Chem. Soc.* 2001, *123*, 12518−12527.

(b) Chong, D.; Georgakaki, I. P.; Mejia-Rodriguez, R.; Sanabria-Chinchilla, J.; Soriaga, M. P.; Darensbourg, M. Y. Electrocatalysis of Hydrogen Production by Active Site Analogues of the Iron Hydrogenase Enzyme: Structure/Function Relationships. *J. Chem. Soc., Dalton Trans.* 2003, 4158−4163. (c) Mejia-Rodriguez, R.; Chong, D.; Reibenspies, J. H.; Soriaga, M. P.; Darensbourg, M. Y. The Hydrophilic Phosphatriazaadamantane Ligand in the Development of H_2 Production Electrocatalysts: Iron Hydrogenase Model Complexes. *J. Am. Chem. Soc.* 2004, *126*, 12004−12014. (d) Felton, G. A. N.; Vannucci, A. K.; Chen, J.; Lockett, L. T.; Okumura, N.; Petro, B. J.; Zakai, U. I.; Evans, D. H.; Glass, R. S.; Lichtenberger, D. L. Hydrogen Generation from Weak Acids: Electrochemical and Computational Studies of a Diiron Hydrogenase Mimic. *J. Am. Chem. Soc.* 2007, *129*, 12521−12530. (e) Gao, S.; Fan, J.; Sun, S.; Peng, X.; Zhao, X.; Hou, J. Selenium Bridged Diiron Hexacarbonyl Complexes as Biomimetic Models for the Active Site of Fe-Fe Hydrogenases. *Dalton Trans.* 2008, 2128−2135.

(22) (a) Ezzaher, S.; Orain, P.-Y.; Capon, J.-F.; Gloaguen, F.; Pétillon, F. Y.; Roisnel, T.; Schollhammer, P.; Talarmin, J. First Insights into the Protonation of Dissymetrically Disubstituted Diiron Azadithiolate Models of the [FeFe]-H_2ases Active Site. *Chem. Commun.* 2008, 2547−2549. (b) Bourrez, M.; Steinmetz, R.; Gloaguen, F. Mechanistic Insights into the Catalysis of Electrochemical Proton Reduction by a Diiron Azadithiolate Complex. *Inorg. Chem.* 2014, *53*, 10667−10673. (c) Esmieu, C.; Berggren, G. Characterizatiuon of a Monocyanide Model of FeFe Hydrogenases Highlighting the Importance of the Bridgehead Nitrogen for Catalysis. *Dalton Trans.* 2016, *45*, 19242−19248. (d) Gloaguen, F. Electrochemistry of Simple Organometallic Models of Iron-Iron Hydrogenases in Organic Solvent and Water. *Inorg. Chem.* 2016, *55*, 390−398. (e) Zhao, P.-H.; Hu, M.-Y.; Li, J.-R.; Ma, Z.-Y.; Wang, Y.-Z.; He, J.; Li, Y.-L.; Liu, X.-F. Influence of the Dithiolate Bridge s on the Structures and Electrocatalytic Performance of Small Bite-Angle PNP-Chelated Diiron Complexes $Fe_2(\mu\text{-xdt})(CO)_4\{k^2\text{-}(Ph_2P)_2NR\}$ Related to [FeFe]-Hydrogenases. *Organometallics* 2019, *38*, 385−394. (f) Rauchfuss, T. B. Diiron Azadithiolates as Models for the [FeFe]-Hydrtogenase Active Site and Paradigm for the Role of the Second Coordination Sphere. *Acc. Chem. Res.* 2015, *48*, 2107−2116.

(23) Raamat, E.; Kaupmees, K.; Ovsjannikov, G.; Trummal, A.; Kütt, A.; Saame, J.; Koppel, I.; Kaljurand, I.; Lipping, L.; Rodima, T.; Pihl, V.; Koppel, I. A.; Leito, I. Acidities of Strong Neutral Bronsted Acids in Different Media. *J. Phys. Org. Chem.* 2013, *26*, 162−170.

(24) Ott, S.; Borgstrom, M.; Kritikos, M.; Lomoth, R.; Bergquist, J.; Akermark, B.; Hammarstrom, L.; Sun, L. Model of the Iron Hydrogenase Active Site Covalently Linked to a Ruthenium Photosensitizer: Synthesis and Photophysical Properties. *Inorg. Chem.* 2004, *43*, 4683−4692. See also ref 10.

(25) See for example: (a) Gloaguen, F.; Lawrence, J. D.; Rauchfuss, T. B.; Béard, M.; Rohmer, M. Bimetallic Carbonyl Thiolates as Functional Models for Fe-Only Hydrogenases. *Inorg. Chem.* 2002, *41*, 6573−6582. (b) Capon, J.-F.; Gloaguen, F.; Schollhammer, P.; Talarmin, J. Electrochemical Proton Reduction by Thiolate-Bridged Hexacarbonyldiiron Clusters. *J. Electroanal. Chem.* 2004, *566*, 241−247. (c) Capon, J.-F.; Gloaguen, F.; Schollhammer, P.; Talarmin, J. Activation of Proton by the Two-Electron Reduction of a Diiron Organometallic Complex. *J. Electroanal. Chem.* 2006, *595*, 47−52. (d) Borg, S. J.; Behrsing, T.; Best, S. P.; Razavet, M.; Liu, X.; Pickett, C. J. Electron Transfer at a Dithiolate-Bridged Diiron Assembly: Electrocatalytic Hydrogen Evolution. *J. Am. Chem. Soc.* 2004, *126*, 16988−16999. (e) Zaffaroni, R.; Rauchfuss, T. B.; Gray, D. L.; De Gioia, L.; Zampella, G. Terminal vs Bridging Hydrides of Diiron Dithiolates: Protonation of $Fe_2(\text{dithiolate})(CO)_2(PMe_3)_4$. *J. Am. Chem. Soc.* 2012, *134*, 19260−19269. (f) Ghosh, S.; Hogarth, G.; Hollingsworth, N.; Holt, K. B.; Kabir, S. E.; Sanchez, B. E. Hydrogenase Biomimetics: $Fe_2(CO)_4(\mu\text{-dppf})$ (μ-pdt) (dppf = 1,1′-bis(Diphenylphosphino)ferrocene) Both a proton Reduction and Hydrogen Oxidation Catalyst. *Chem. Commun.* 2014, *50*, 945−947.

(26) Mariani, A.; Bartoli, A.; Atwal, M.; Lee, K. C.; Austin, C. A.; Rodriguez, R. Differential Targetting of Human Topoisomerase II Isoforms with Small Molecules. *J. Med. Chem.* 2015, *58*, 4851−4856.

(27) Wu, W.; Wu, W.; Ji, S.; Guo, H.; Song, P.; Han, K.; Chi, L.; Shao, J.; Zhao, J. Tunning the Emission Properties of Cyclometallated Platinum(II) Complexes by Intramolecular electron-Sink/Arylethynylated Ligands and its Applications for Enhanced Luminescent Oxygen Sensing. *J. Mater. Chem.* 2010, *20*, 9775−9786.

(28) Wang, S.-B.; Jin, P.; Li, F.-N.; Quan, Z.-S. Synthesis and Anticonvulsant Activity of Novel Purine Derivatives. *Eur. J. Med. Chem.* 2014, *84*, 574−583.

(29) (a) Dilek Celik, G.; Disli, A.; Oner, Y.; Acik, L. Synthesis of Some Novel Amino and Thiotetrazole Purine Derivatives and Investigation of their Antimicrobial Activity and DNA Interactions. *Med. Chem. Res.* 2013, *22*, 1470−1479. (b) Kim, B. Y.; Ahn, J. B.; Lee, H. W.; Kang, S. K.; Lee, J. H.; Shin, J. S.; Ahn, S. K.; Hong, C. I.; Yoon, S. S. Synthesis and Biological Activity of Novel Substituted Pyridines and Purines Containing 2,4-Thiazolidinedione. *Eur. J. Med. Chem.* 2004, *39*, 433−447.

(30) (a) Naus, P.; Votruba, I.; Hocek, M. Covalent Analogues of DNA Base-Pairs and Triplets VII. Synthesis and Cytostatic Activity of Bis(purin-6-yl)acetylene and − diacetylene Nucleosides. *Collect. Czech. Chem. Commun.* 2004, *69*, 1955−1970. (b) Mathew, S. C.; By, Y.; Berthault, A.; Virolleaud, M. A.; Carrega, L.; Chouraqui, G.; Commeiras, L.; Condo, J.; Attolini, M.; Gaudel-Siri, A.; Ruf, J.; Rodriguez, J.; Parrain, J. L.; Guieu, R. Expeditious Synthesis and Biological Evaluation of New C-61,2,3-triazole Adenosine Derivatives A1 Receptor Antagonists or Agonists. *Org. Biomol. Chem.* 2010, *8*, 3874−3881.

(31) Buck, I.; Reese, C. B. An Unambiguous Synthesis of Adenylsuccinic Acid and its constituent Nucleoside. *J. Chem. Soc., Perkin Trans. 1* 1990, 2937−2942.

(32) Claudio-Montero, A.; Pinilla-Macua, I.; Fernandez-Calotti, P.; Sancho-Mateo, C.; Lostao, M. P.; Colomer, D.; Grandas, A.; Pastor-Anglada, M. Fluorescent Nucleoside Derivatives a Tool for the Detection of Concentrative Nucleoside Transporter Activity Using Confocal Microscopy and Flow Cytometry. *Mol. Pharmaceutics* 2015, *12*, 2158−2166.

(33) Hocek, M.; Holy, A.; Votruba, I.; Dvorakova, H. Synthesis and Cytostatic Activity of Substituted 6-Phenylpurine Bases and Nucleosides: Application of the Suzuki-Miyaura Cross-Coupling Reactions of 6-Chloropurine Derivatives with Phenylboronic Acids. *J. Med. Chem.* 2000, *43*, 1817−1825.

(34) Ast, S.; Fischer, T.; Mueller, H.; Mickler, W.; Schwichtenberg, M.; Rurack, K.; Holdt, H. J. Integration of the 1,2,3-Triazole Click Motif as a Potent Signalling Element in Metal Ion Responsive Fluorescent Probes. *Chem. - Eur. J.* 2013, *19*, 2990−3005.

(35) Doisneau, G.; Balavoine, G.; Fillebeen-Khan, T. Synthesis and Some Reactions of Ferrocenylacetylenes. *J. Organomet. Chem.* 1992, *425*, 113−117.

(36) Rausch, M. D.; Siegel, A. Organometallic pi-Complexes. XVII. Formation of 2-Ferrocenylbenzofuran and some Acetylenic Derivatives of Ruthenocene. *J. Org. Chem.* 1969, *34*, 1974−1976.

(37) Lo Sterzo, C.; Miller, M. M.; Stille, J. K. Use of Palladium-catalyzed Coupling Reaction in Synthesis of Homobimetallic Dimers: Preparation of [Bis(cyclopentadienyl)acetylene]metal Complexes and their Reaction with Dicobalt Octacarbonyl. Evidence for Formation of Dihydrido Species in Diiron Complexes. *Organometallics* 1989, *8*, 2331−2337.